N71-19245

OPTIMUM PRESSURE VESSEL DESIGN BASED ON FRACTURE MECHANICS AND RELIABILITY CRITERIA

Ewald Heer, et al

California Institute of Technology
Pasadena, California

February 1970

Technical Memorandum 33-470

Optimum Pressure Vessel Design Based on Fracture Mechanics and Reliability Criteria

Ewald Heer

Jann-Nan Yang

PREFACE

The work described in this report was performed by the Engineering Mechanics Division of the Jet Propulsion Laboratory.

ACKNOWLEDGMENT

CONTENTS

ABSTRACT

Spacecraft structural systems and subsystems are subjected to a number of qualification tests in which the proof loads are chosen at some level above the simulated loads expected during the space mission. Assuming fracture as prime failure mechanism, and allowing for time effects due to cyclic and sustained loadings, this paper treats an optimization method in which the statistical variability of loads and material properties are taken into account, and in which the proof load level is used as an additional design variable. In the optimization process, the structural weight is the objective function while the total expected cost due to coupon testing for material characterization, due to failure during proof testing, and due to mission degradation is a constraint. Numerical results indicate that for a given expected cost constraint, substantial weight savings and improvements of reliability can be realized by proof testing.

I. INTRODUCTION

Structural design is the sizing and synthesizing of structural elements in space for certain intended purposes. Although the purposeful geometrical arrangement of the structural elements can be accomplished with adequate, better, or optimum results, in structural optimization it is usually assumed that the geometrical configuration of the structure is given as constant. It is also assumed that the design and optimization are performed with the sizes of the individual structural elements being used as generalized coordinates. These coordinates are varied to determine, within specified constraints, those values that will yield an extremism of a given objective function.

The objective function to be extremized may be structural weight, cost, reliability, etc. In many cases, it is necessary to determine how weak the structural elements can be designed without resulting in too many failures. In determining this weakness, one should recognize that structural loads and structural strength properties are satistical variables and, therefore, it is not possible to eliminate all structural failures. There will always be a finite probability of structural failure, and the most one can hope for is to limit this probability to a tolerable value. Thus, the

desire to set the probability of failure as low as possible, i.e., to set the structural strength as high as possible, is unfortunately countered by the necessity of reducing the structural weight to a minimum and/or by the necessity of keeping costs within tolerable limits. It follows that an increase in structural reliability (probability of structural survival) must usually be paid for by an increase in weight, or cost, or both.

Once the structural is designed and built, the question then arises concerning the reliability of the particular structure. The answer to this question is not simple. The most careful analysis and design before building the structure, taking into account the statistical variabilities of material properties, loads, and other measurable parameters, become meaningless when, during the manufacturing process, an error is committed that was not allowed for in the design. In a statistical sense, such errors could be allowed for in the design procedure if estimates of their probability of occurrences and severity are included in the reliability evaluation of the structure. However, for structural systems involving new processes and techniques, such estimates are by necessity very vague because of the lack of information on which to base them.

Therefore, one is left with two essential contributions to the statistical strength variability of the structure: (1) the statistical variability of measurable quantities, such as material properties, dimensions, etc., and (2) the statistical variability of chance events, such as gross errors during design, gross errors during fabrication, etc. In this report, only the statistical strength variability due to measurable quantities is considered. It can be shown later that as far as structural reliability is concerned this consideration is on the safe side. Additional information, which may become available regarding chance events, can be incorporated in the structural strength distributions without causing a change in the basic approach as set forth in this report.

Spacecraft structural systems and subsystems are subjected to a number of qualification tests in which the structural components must withstand specified environments (proof loads) that are intended to simulate the various types of induced stresses at some level above those expected during the space mission. The purpose of these proof-load tests is to eliminate those structures or structural components that are too weak.

It is clear that after the structural system or subsystem has passed the proof-load tests, its statistical strength characteristics are radically changed. For instance, assuming negligible time effects during proof-stress application, the statistical strength distribution, at the particular point under consideration in the structure after the test, will be truncated at the lower end up to the proof-stress level. A similar statement is true for the proof load applied to a structure and the resulting truncated overall structural strength distribution. This truncation eliminates, through the proof test, precisely that portion of the strength distribution that is least known and that has the greatest interaction with the applied load distribution (Fig. 1). Reference 1 contains some implications of screening out weak elements with a proof test when the proof-stress distributions are similar, dissimilar, and identical to the applied-load induced stresses; Ref. 1 also includes some simple aspects of optimum designs.

Reference 2 introduces the proof-load test level as a design parameter. It is shown in Fig. 1

that the choice of the proof-load test level considerably influences the reliability of the structure. In the associated optimization problem, with weight as the objective function and total expected cost as a constraint, Ref. 2 indicates that an optimum proof-load test level can usually be obtained with an increase of reliability and a decrease in weight as compared to conventional optimum designs in which the proof load is not considered in the reliability evaluation. In Ref. 2, the expected cost consisted of the expected cost of mission failure due to structural failure plus the expected cost of failed subsystems (or components) during proof-load testing.

Frequently the optimum proof-load test level is considerably different from the mean structural strength. Since the probability density function of the structural strength is usually only known with a certain degree of confidence close to the mean strength, it would be necessary, in such cases, to establish, through extensive specimen testing, strength density function at points far apart from its mean. This effort can add substantial additional costs to the overall evaluation process if the strength density function is not available.

In Ref. 3, this additional cost item has been allowed for by the fact that a linear increase of testing cost was assumed with an increase of the difference between mean strength and proof-load test level. The effect of this additional cost is an increasing tendency to reduce the difference between mean strength and proof-load test level as the additional testing cost is increased.

In this report, which includes the essential aspects of Ref. 4, an approach similar to that in Ref. 3 is taken in the optimization process. This approach also includes in the expected cost constraint, the cost of establishing the truncated strength distribution function by specimen testing. Fracture mechanics dealing with essentially brittle fracture has been chosen here as an area of application, since fracture mechanics design, as compared to other structural design approaches in which considerable bulk yield occurs before failure, tends to be more susceptible to statistical strength variations. The wide scatter of the results of tests leading to failure is assumed to be

an inherent property of the material and is treated as such for the purposes of this report, which concerns the investigation of trends of behavior rather than absolutes. A detailed discussion of various probability models for the characterization of material properties and their implications with respect to specimen size is given in Ref. 5. This report also considers volume effects and time effects, such as fatigue due to cyclic loading and flaw growth due to sustained loading.

In spacecraft structural design, fracture mechanics concepts can be most readily and meaningfully applied to pressure vessel subsystems. This report is mainly concerned with pressure vessel design optimization, although the concepts put forth are equally applicable in other areas of design. As will become apparent from this investigation, this approach tends to become more meaningful as the systems, subsystems, and components become less expensive relative to the overall project cost.

II. FRACTURE MECHANICS CONCEPTS

Fracture mechanics treats failures that occur because of the presence of existing flaws in the material. The stress intensifications that are induced at the edges of a flaw correspondingly increase locally the stored energy. If this stored energy just ahead of the flaw tip becomes larger than the energy needed to create the new surfaces resulting from an extension of the flaw tip, then the flaw increases until energy balance has been restored (Ref. 6). If the applied stress is high enough, or if additional energy in some other form is applied, the energy balance at the flaw tip will not be restored and catastrophic failure will occur. Hence, for a given flaw size, an applied critical stress exists that causes rapid propagation of the flaw without further increase of the applied stress. In ductile materials that generally have small initial flaw sizes, this critical stress approaches the material yield strength, while in brittle materials the critical stresses are usually less than the yield strength of the material.

The original work in fracture mechanics is associated with the name of Griffith, who solved the problem of a flaw in an elastic material (Ref. 7). Griffith's theory has been generalized by Irwin (Ref. 8) to include plastic deformations at the crack tip. Recently, a number of authors, e. g.,

the authors of Refs. 9 and 10, have extended these investigations to include (1) the effects of the proximity of flaws to the material surface, (2) the effects of sustained loading, and (3) the effects of cyclic loading. Mainly as a result of these works, fracture mechanics can be put on a quantitative basis by the following equation:

$$\left(\frac{a}{Q}\right)_{cr} = \frac{c}{\pi M_k^2}\left(\frac{K_{Ic}}{R}\right)^2 \tag{1}$$

where a is the minor semiaxis of an elliptically shaped flaw at onset of rapid fracture as shown in Fig. 2. Figure 3 shows that Q is a flaw shape parameter that depends on the ratio of applied stress to yield stress. The subscript cr denotes the critical state at the outset of rapid fracture. On the right side of Eq. (1), c is a numerical correction factor that varies with the location of the flaw with respect to the free surface. For surface flaws, c = 0.83 and for internal (completely embedded) flaws, c = 1.00 (Fig. 2). The factor M_k indicates the effect of flaw size compared to that of material thickness. Figure 4 shows typical curves for M_k and experimental values as functions

of the ratio of flaw size to material thickness h. The fracture toughness K_{Ic} indicates the capability of a material to resist fracture in the presence of a flaw under an applied tensile stress R (resisting strength) perpendicular to the flaw plane; it is sometimes called the critical stress intensity factor. The subscript I refers to the opening mode of fracture for plane strain conditions. The value of K_{Ic} generally depends upon such factors as heat treatment, temperature, etc. Figure 5 gives a typical curve and some experimental values of K_{Ic} as a function of temperature. The fracture toughness is higher for the plane stress fracture mode than for the plane strain fracture mode, with some transition values between these two modes. Figure 6 shows a typical variation of the fracture toughness with thickness h, where K_c is the fracture toughness referring to the opening mode of fracture for plane stress conditions.

If the applied stress S perpendicular to the plane of a flaw is less than the critical fracture stress R, Eq. (1) has the form

$$\frac{a}{Q} = \frac{c}{\pi M_k^2}\left(\frac{K_I}{S}\right)^2$$

where K_I is any applied noncritical plane strain intensity factor. Figure 7 shows schematically the applied stress as a function of the flaw size parameter a/Q along constant lines of K_{Ic} and K_I.

Equations (1) and (2) are the basic equations describing the relationship between crack size and applied stress for the simplest case; i.e., that of a single, short-time stress application at a constant temperature in an inert environment. The design of structures requires additional considerations beyond these. Environmental effects such as temperature, cyclic loading, and corrosion have a pronounced influence on the fracture characteristics of structures. Many materials fracture not only when a certain critical stress is reached but also at relatively low stresses after being subjected for a certain time to sustained loading, or after a certain number of load cycles, or any combination

thereof. These are time-dependent cases in which not only the level of applied stress is of importance but also the duration of stress or the number of applied stress cycles. Such cases involve subcritical flaw growth; i.e., the slow growth of a flaw until it reaches its critical value and catastrophic fracture occurs. Subcritical flaw growth is conveniently indicated by curves of K_I/K_{Ic} versus time or cycles of loading to failure that are determined from tests on preflawed specimens by a change in both the initial flaw size and the applied stress. Figure 8 shows typical curves for cyclic loading, and Fig. 9 gives typical curves for sustained loading.

The curves for sustained stress applications have characteristic trends showing that for a given material and environmental condition practically no flaw growth occurs until a certain threshold ratio of K/K_{Ic} is reached. In Fig. 9, this threshold is approximately 0.9 for titanium and 0.75 for aluminum in a liquid nitrogen environment.

The effects of corrosive and oxidizing environments vary considerably for different materials, but they usually lower the threshold stress intensity values. Temperature also affects the breakdown process in a number of ways. For instance, as shown in Fig. 5, K_{Ic} depends on temperature, and corrosion and oxidation are usually accelerated with increasing temperature.

A typical schematic design case is shown in Fig. 10. It is assumed that the loading history is as shown in Fig. 10a, in which a proof load is initially applied at time T_A, then a cyclic load is applied between times T_B and T_C, and then a sustained load between times T_C and T_D. Also, it is assumed that the maximum initial embedded flaw size parameter is (a_i/Q_i). The proof load, being of short duration, has a negligible effect on subcritical flaw growth. The cyclic and sustained loads, however, determine the maximum allowable operating load as indicated by the arrows in Fig. 10b. During cyclic loading, the flaw increases from point ① to point ② (Fig. 10b), and under sustained loading it increases from point ② to point ③ when the critical flaw size for the applied operating load is reached and fracture takes place.

This design process requires knowledge of the largest initial embedded flaw size, which is usually not available. By proof loading the structure, it is established that the largest initial flaw is not larger than that indicated by point ④ in Fig. 10; however, no knowledge is provided as to how much smaller it might be.

The preceding discussion indicates that to fully characterize the material properties, all the possible environmental and loading conditions must be taken into account and extensive experimental data must be generated. This is not only time-consuming; it can also become intolerably expensive.

III. STATISTICAL ASPECTS OF FRACTURE

It is recognized that the strength of material is a random variable. In fact, the statistical properties of material strength were investigated extensively (Refs. 11-15) under one-dimensional stress-field applications. In fracture mechanics, the major reason for the statistical variation of the material strength is attributed to the statistical variation of the embedded flaw sizes that appear to be inherent characteristics of the material. It is mainly due to this fact that the strength of the material is far below the theoretical value computed from atomic bond considerations.

Without essential loss of generality, a two-dimensional stress field (plane stress), as commonly associated with the stresses in thin-walled pressure vessels and other thin-walled structures, is assumed here for the derivation of the statistical distribution of the resisting strength of the structure.

Let the structure be divided into small material volume elements, each containing one flaw. Equations (1) and (2) are then written as

$$R_j = \left(\frac{c}{\pi}\right)^{1/2} \frac{K_{Ic}}{M_k} a_j^{-1/2} = A_c a_j^{-1/2} \qquad (3)$$

$$S_j = \left(\frac{c}{\pi}\right)^{1/2} \frac{K_I}{M_k} a_j^{-1/2} = A a_j^{-1/2} \qquad (4)$$

in which R_j and S_j are, respectively, the resisting stress and applied stress normal to the plane of the flaw of size parameter $a_j = (a/Q)_j$ contained in the jth volume element V_j.

Since a_j has by far the largest statistical dispersion as compared to the statistical dispersion of the other parameters in Eqs. (3) and (4), it is assumed that A_c and A are deterministic constants.

Under the weakest-link hypothesis, which states that failure of the structure occurs when any one of the material elements is subjected to its critical stress, the statistical distribution of the resisting strength of the structure can be derived from that of R_j, whereas the statistical distribution of R_j can be determined from that of a_j by a transformation of Eq. (3). The present state of technology does not allow, in most cases, the direct measurement of the distribution of a_j. Therefore, the distribution of R_j is determined from results of uniaxial tensile tests of specimens, henceforth referred to as coupon tests.

Let S and R be, respectively, the applied load to and the resisting strength of the structure, and let $S\phi_{j1}$ and $S\phi_{j2}$ be the analyzed principal stresses at V_j due to the application of S. Here, ϕ_{j1} and ϕ_{j2} are functions of the spatial coordinates and stiffness properties defining the structure. If θ_j is the angle between the plane of the flaw contained in V_j and the principal stress $S\phi_{j1}$, the applied stress normal to the plane of the flaw is then

$$S_j = S\phi_{j1} \cos^2 \theta_j + S\phi_{j2} \sin^2 \theta_j \qquad (5)$$

It is reasonable to assume that the a_j, $j = 1, 2, 3, \cdots, m$ are statistically independent and identically distributed and that the angles θ_j, $j = 1, 2, 3, \cdots, m$ are also statistically independent and uniformly distributed between 0 and $\pi/2$. Thus,

$$f_{\theta_j}(x) = f_\theta(x) = \frac{2}{\pi}, \qquad 0 \leq x \leq \frac{\pi}{2} \qquad (6)$$

$$= 0 \qquad \text{otherwise}$$

in which $f_\theta(x)$ is the probability density function of θ.

The probability of failure of the entire structure due to a deterministic applied load S is

$$p_f = P[R \leq S] = 1 - \prod_{j=1}^{m} \left\{ 1 - P[R_j \leq S_j] \right\} \qquad (7)$$

where S_j is the applied stress due to S normal to the plane of a_j and $P[E]$ is the probability of occurrence of the event E. Equation (7) simply states that the survival of the structure implies the survival of each volume element.

The unconditional probability of the event $[R_j \leq S_j]$ for given $\theta_j = \psi$, $P[R_j \leq S_j | \theta_j = \psi]$, follows from Eq. (5),

$$P[R_j \leq S_j | \theta_j = \psi] =$$

$$P[R_j \leq S\phi_{j1} \cos^2 \psi + S\phi_{j2} \sin^2 \psi] \qquad (8)$$

For uniaxial tensile tests (coupon tests) in which $\phi_{j1} = 1$ and $\phi_{j2} = 0$, Eq. (8) yields

$$P[R_j \leq S_j | \theta_j = \psi] = P\left[\frac{R_j}{\cos^2 \psi} \leq S \right] = F_{R_{ju}}(S) \qquad (9)$$

where $F_{R_{ju}}(x)$ is the distribution function of the uniaxial tensile strength for the jth volume element, and

$$R_{ju} = \frac{R_j}{\cos^2 \psi} \qquad (10)$$

From experience, e.g., Refs. 5 and 11-15, the distribution function $F_{R_c}(x)$ of the uniaxial tensile strength R_c of the coupon specimen with volume V_c can be represented by the Weibull distribution

$$F_{R_c}(x) = 1 - \exp\left\{ -\frac{V_c}{v}\left(\frac{x - x_\mu}{x_0} \right)^k \right\}, \qquad x \geq x_\mu \qquad (11)$$

in which x_μ, x_0 and k are parameters characterizing the particular material and v is the unit volume.

The distribution function of the uniaxial tensile strength R_{ju} of the jth volume element follows from Eq. (11) and Refs. 1, 5, and 10-12,

$$F_{R_{ju}}(x) = 1 - \exp\left\{ -\frac{V_j}{v}\left(\frac{x - x_\mu}{x_0} \right)^k \right\}, \qquad x \geq x_\mu \qquad (12)$$

With the aid of Eqs. (9), (10), and (12), Eq. (8) yields

$$P[R_j \leq S_j | \theta_j = \psi] =$$

$$1 - \exp\left\{ -\frac{V_j}{v}\left[\frac{S(\phi_{j1} + \phi_{j2} \tan^2 \psi) - x_\mu}{x_0} \right]^k \right\} \qquad (13)$$

The unconditional probability can be obtained from Eqs. (6) and (13) as follows:

$$P[R_j \leq S_j] = 1 - \frac{2}{\pi} \int_0^{\pi/2} \exp\left\{ -\frac{V_j}{v}\left[\frac{S(\phi_{j1} + \phi_{j2} \tan^2 \psi) - x_\mu}{x_0} \right]^k \right\} d\psi, \qquad S(\phi_{j1} + \phi_{j2} \tan^2 \psi) \geq x_\mu \qquad (14)$$

The distribution function cf the structural strength $F_R(S)$ follows then from Eqs. (7) and (14) as

$$F_R(S) = P[R \leq S] = 1 - \frac{2}{\pi} \prod_{j=1}^{m} \int_0^{\pi/2} \exp\left\{-\frac{V_j}{v}\left[\frac{S\left(\phi_{j1} + \phi_{j2}\tan^2\psi\right) - x_\mu}{x_0}\right]^k\right\} d\psi, \qquad S\left(\phi_{j1} + \phi_{j2}\tan^2\psi\right) \geq x_\mu$$

(15)

The integration with respect to ψ in Eq. (15), in general, cannot be carried out analytically. If it is assumed that the mean value $\overline{\theta}_j = \pi/4$ as an approximation for the orientation θ_j, Eq. (15) yields

$$F_R(S) = 1 - \prod_{j=1}^{m} \exp\left\{-\frac{V_j}{v}\left[\frac{S(\phi_{j1} + \phi_{j2}) - x_\mu}{x_0}\right]^k\right\}, \qquad S(\phi_{j1} + \phi_{j2}) \geq x_\mu$$

(16a)

with the approximation

$$F_R(S) = 1 - \exp\left\{-\int_V \frac{1}{v}\left[\frac{S(\phi_1 + \phi_2) - x_\mu}{x_0}\right]^k dv\right\}, \qquad S(\phi_1 + \phi_2) \geq x_\mu$$

(16b)

The last approximation leading to Eq. (16) is equivalent to the criterion that fracture occurs whenever the sum of the two principal stresses exceeds some critical constant value C; i.e.,

$$S\phi_1 + S\phi_2 = C$$

(17)

For a spherical pressure vessel in which approximately $\phi_1 = \phi_2 = \phi =$ constant, the distribution function of the vessel strength becomes

$$F_R(S) = 1 - \exp\left\{-\frac{V}{v}\left(\frac{2S\phi - x_\mu}{x_0}\right)^k\right\}, \qquad 2S\phi \geq x_\mu$$

(18)

in which V is the total material volume of the pressure vessel.

It follows from Eqs. (16) and (18) that the distribution function of the strength of the entire structure under two-dimensional stress-field applications is also a Weibull distribution in which the parameters x_μ, x_0 and k can be estimated from coupon tests. The estimation of x_μ, x_0 and k can be obtained from the results of coupon tests by the method of moments; i.e., the population mean m_1, the variance m_2 and the third central moment m_3 are, respectively, equated to the unbiased sample mean $\overline{m}_1$, the variance $\overline{m}_2$ and the third central moment $\overline{m}_3$, where

$$\left. \begin{aligned} m_1 &= x_\mu + x_v \Gamma\left(1 + \frac{1}{k}\right) \\[2mm] m_2 &= x_v^2\left[\Gamma\left(1 + \frac{2}{k}\right) - \Gamma^2\left(1 + \frac{1}{k}\right)\right] \\[2mm] m_3 &= x_v^3\left[\Gamma\left(1 + \frac{3}{k}\right) - 3\Gamma\left(1 + \frac{2}{k}\right)\Gamma\left(1 + \frac{1}{k}\right) + 2\Gamma^3\left(1 + \frac{1}{k}\right)\right] \end{aligned} \right\}$$

(19a)

and

$$\overline{m}_1 = \frac{1}{n}\sum_{j=1}^{n} Y_j$$

$$\overline{m}_2 = \frac{1}{n-1}\sum_{j=1}^{n}(Y_j - \overline{m}_1)^2 \left.\rule{0pt}{90pt}\right\}\quad (19b)$$

$$\overline{m}_3 = \frac{n}{(n-1)(n-2)}\sum_{j=1}^{n}(Y_j - \overline{m}_1)^3$$

Here

$$x_\nu = x_0\left(\frac{V_c}{\nu}\right)^{-1/k}$$

n is the number of coupon tests, Y_j is the observation of the jth test result, and $\Gamma(\cdot)$ is the gamma function. Equating Eq. (19a) to Eq. (19b), one obtains three equations for the determination of x_μ, x_0 and k. Other methods of estimation can be found, e. g., in Ref. 10.

IV. TIME EFFECTS

In Section II, it was mentioned that during cyclic loading, and during sustained loading above a certain threshold value, subcritical flaw growth is expected. In this report, it is assumed that the time relationships of these subcritical flaw growths are representable by deterministic relations that are determined experimentally from tests on pre-flawed coupons by varying both the flaw size and the applied stress. As can be seen from such typical data as shown in Figs. 8 and 9, the changes of the ratios K_I/K_{Ic} for the cyclic and the sustained case, respectively, can be written in the general form

$$\frac{K_I}{K_{Ic}} = W(n) \tag{20}$$

$$\frac{K_I}{K_{Ic}} = U(t) \tag{21}$$

in which n indicates the number of cycles to failure and t is the time to failure. The functions W(n) and U(t) are monotonically decreasing functions of their arguments.

From Eqs. (3), (4), (20) and (21), one obtains

$$\frac{S_{cj}}{R_{cj}} = W(n) \tag{22}$$

$$\frac{S_{sj}}{R_{sj}} = U(t) \tag{23}$$

in which S_{cj} and S_{sj} are, respectively, the stresses due to cyclic and sustained loading. The terms R_{cj} and R_{sj} are the corresponding strengths of the jth element before the application of S_{cj} and S_{sj}.

The function U(t) usually has a characteristic shape that can be approximated by an exponential decay to the threshold value. Thus

$$U(t) = b + re^{-t/\tau} \tag{24}$$

where b and τ represent the threshold value and a characteristic time, respectively, and t denotes the time to fracture in log scale. The parameters b, τ and r are material properties depending on the environmental conditions such as temperature, etc.

It should be noted that the above equations are valid for a particular volume element; i.e., *for a given stress distribution they are also valid for*

the weakest volume element. However, since the structural strength R can be assumed to be equal to the strength of the weakest material volume element, the strength deterioration of the structure is equivalent to the strength deterioration of the weakest volume element.

In this report it is assumed that subcritical flaw growth, i.e., the time-dependent deterioration of structural strength is negligible under the short duration proof-load test. This assumption seems justified on the basis of the following two considerations.

First, during proof loading the embedded flaws in the structure may undergo some growth. If at the instant of unloading from the proof-load level the structure has not failed, then the maximum flaw in the structure at that moment was less than the critical flaw associated with the proof-load level. During unloading, additional flaw growth may occur. However, based on available test results for rates of unloading commonly employed, e.g., during pressure vessel proof-load testing, this additional flaw growth is either not detectable or it is negligibly small.

Second, during proof loading, some rearrangement of the statistical flaw size distribution may take place. To this time, it has not been possible to assess the effect of such a change in flaw size distribution. Although in some cases (depending on the degree of ductility of the material) it can be argued that proof loading has a beneficial effect on the subsequent strength behavior of the structure because of the "shakedown" phenomena, the redistribution effect on ultimate strength is probably negligible compared to other effects.

Based on the above assumptions and considering a loading history as shown in Fig. 10, the deteriorated strength of the structure, after application of the proof load S_0 and n loading cycles

with amplitude S_c, can be derived from Eqs. (3), (4), and (22) in the following form:

$$R(n) = \frac{S_c}{W\left[W^{-1}\left(\frac{S_c}{R_0}\right) - n\right]} \quad \text{for } W^{-1}\left(\frac{S_c}{R_0}\right) - n > 0$$

$$= 0 \qquad \text{otherwise} \qquad (25)$$

where R_0 is the structural strength after proof-load application. Similarly, by the use of Eqs. (3), (4), (23), and (24), the deteriorated strength after application of the sustained load with amplitude S_s for a time period T following application of n loading cycles with amplitude S_c is

$$R(T) = \frac{S_s}{U\left[U^{-1}\left(\frac{S_s}{R(n)}\right) - T\right]} \quad \text{for } 1 > \frac{S_s}{R(n)} > b$$

$$U^{-1}\left(\frac{S_s}{R(n)}\right) - T > 0$$

$$= R(n) \qquad \text{for } b \geq \frac{S_s}{R(n)}$$

$$= 0 \qquad \text{otherwise} \qquad (26)$$

In Eqs. (25) and (26), $W^{-1}(x)$ and $U^{-1}(y)$ are the inverse functions of $W(x)$ and $U(y)$ in Eqs. (22) and (23), which represent the number of cycles-to-failure associated with $S_c/R_0 = x$ and the time-to-failure associated with $S_s/R(n) = y$, respectively. Expressions similar to those in Eqs. (25) and (26) can be derived if the loading sequence of S_c and S_s is interchanged.

V. PROBABILITY OF FAILURE

Those structures that have passed the proof-load test are to be used in actual mission applications. The original strength distribution for these vessels has been changed by the proof-load test. This change must be accounted for in the reliability evaluation. If R_0 is the structural strength after the application of the proof load S_0, then the structural strength distribution is given by the conditional probability

$$F_{R_0}(x) = P\left[R \le x | R > S_0\right] = \frac{F_R(x) - F_R(S_0)}{1 - F_R(S_0)} \qquad for\ x \ge S_0 \tag{27}$$

Use of Eq. (16b) gives

$$F_{R_0}(x) = 1 - \exp\left\{-\frac{1}{v}\int_V\left[\left(\frac{x(\phi_1 + \phi_2) - x_\mu}{x_0}\right)^k - \left(\frac{S_0(\phi_1 + \phi_2) - x_\mu}{x_0}\right)^k\right]dv\right\}$$

$$for\ x(\phi_1 + \phi_2) \ge S_0(\phi_1 + \phi_2) \ge x_\mu \tag{28}$$

Equation (28) is valid when $x(\phi_1 + \phi_2)$ is proportional to $S_0(\phi_1 + \phi_2)$. If this proportionality does not hold, then the *strength distribution*, after application of S_0, is given by

$$F_{R_0}(x) = 1 - \exp\left\{-\frac{1}{v}\int_V\left[\left(\frac{x(\phi_1 + \phi_2) - x_\mu}{x_0}\right)^k - \left(\frac{S_0(\overline{\phi}_1 + \overline{\phi}_2) - x_\mu}{x_0}\right)^k\right]dv\right\}$$

$$for\ x(\phi_1 + \phi_2) \ge S_0(\overline{\phi}_1 + \overline{\phi}_2) \ge x_\mu \tag{29}$$

To simplify the algebra, Eq. (28) is used in what follows without essential loss of generality.

For a spherical pressure vessel in which approximately $\phi_1 = \phi_2 = \phi = $ constant,

$$F_{R_0}(x) = 1 - \exp\left\{-\frac{V}{v}\left[\left(\frac{2x\phi - x_\mu}{x_0}\right)^k - \left(\frac{2S_0\phi - x_\mu}{x_0}\right)^k\right]\right\}$$

$$\text{for } x \geq S_0 \quad (30)$$

The probability of structural failure p_0 due to the proof load S_0 follows then from Eq. (16b) as

$$p_0 = F_R(S_0) =$$

$$1 - \exp\left\{-\frac{1}{v}\int_V\left[\frac{S_0(\phi_1 + \phi_2) - x_\mu}{x_0}\right]^k dv\right\} \quad (31)$$

and for the spherical pressure vessel this becomes

$$p_0 = 1 - \exp\left\{-\frac{V}{v}\left(\frac{2S_0\phi - x_\mu}{x_0}\right)^k\right\} \quad (32)$$

Let p_c be the probability of structural failure due to n cycles of the cyclic load S_c after S_0 has been applied, and let p_{cs} be the probability of structural failure due to the sustained load S_s for a period of time T, given that the structure has survived S_c. Then, it follows from Eqs. (22) and (23) that

$$p_c = P\left[\frac{S_c}{R_0} \geq W(n)\right]$$

$$= \int_0^\infty F_{R_0}\left(\frac{x}{W(n)}\right)f_{S_c}(x)\,dx \quad (33)$$

and

$$p_{cs} = P\left[\frac{S_s}{R(n)} \geq U(T)\,\middle|\,R(n) > 0\right]$$

$$= \int_0^\infty F_{R(n)}\left(\frac{x}{U(T)}\,\middle|\,R(n) > 0\right)f_{S_s}(x)\,dx \quad (34)$$

In Eqs. (33) and (34), $f_{S_c}(x)$ and $f_{S_s}(x)$ are, respectively, the probability density functions

of S_c and S_s, and $F_{R_0}(\cdot)$ is given by Eqs. (28) or (30).

The conditional distribution function

$$F_{R(n)}(x/U(T)\,|\,R(n) > 0)$$

of $R(n)$ given $R(n) > 0$ can be obtained from Eq. (25) as follows:

$$F_{R(n)}\left(x\,|\,R(n) > 0\right) = P\left[R(n) \leq x\,|\,R(n) > 0\right]$$

$$= P\left[\frac{S_c}{W\left[W^{-1}\left(\frac{S_c}{R_0}\right) - n\right]} \leq x\right]$$

$$= \int_0^\infty F_{R_0}\left(\frac{y}{W\left[W^{-1}\left(\frac{y}{x}\right) + n\right]}\right)f_{S_c}(y)\,dy$$

$$(35)$$

Substitution of Eq. (35) into Eq. (34) yields

$$p_{cs} =$$

$$\int_0^\infty \int_0^\infty F_{R_0}\left(\frac{y}{W\left[W^{-1}\left(\frac{yU(T)}{x} + n\right)\right]}\right)f_{S_c}(y)f_{S_s}(x)\,dy\,dx$$

$$(36)$$

in which it should be realized that $W^{-1}(x) = 0$ for $x \geq 1$ and $F_{R_0}(x) = 0$ for $x < S_0$.

The probability of structural failure due to the application of sustained loading S_s for a period of time T after passing the proof load test, i.e., without applying the cyclic loading S_c, is

$$p_s = P\left[\frac{S_s}{R_0} \geq U(T)\right] = \int_0^\infty F_{R_0}\left(\frac{x}{U(T)}\right)f_{S_s}(x)\,dx \quad (37)$$

The probability of failure p_{sc} due to n cycles of S_c, given that the structure has survived S_s for a period T after S_0, can be obtained in a similar fashion as the probability of failure p_{cs}.

VI. OPTIMIZATION

Obtaining the best possible performance, or the least possible cost, or the least possible weight, etc., is an integral part of every structural design. The optimization task is to find the values of the controllable parameters, subject to the various constraints, that make a desired objective function an extremum. In this report, the objective function to be optimized is the structural weight or the statistically expected cost; i.e., the mean cost due to coupon testing, proof testing and mission degradation. The structural weight is expressible in terms of the physical parameters such as density and structural dimensions, and the cost items are expressible in terms of the proof-load test levels, as well as the physical parameters. It is the objective of the present optimization process to determine those proof-load test levels and physical parameters which yield minimum expected cost, or which yield minimum weight subject to an expected cost constraint.

Coupon testing has as its prime purpose the characterizations of the statistical strength properties of the structural material. The efforts and costs that must be expended to establish, with sufficient confidence, the material strength distributions for one or more environmental conditions can

be substantial. In particular, if this information is required at the tail end of the distributions, the number of coupon tests and the associated cost soon become intolerably high. Thus, in the overall cost picture, the required expenditures for material characterization should be taken into account.

As indicated by Eq. (28), the truncated structural strength distribution $F_{R_0}(x)$, after the application of the proof load, is zero for strength values less than S_0. Therefore, the lower tail of the original strength distribution $F_R(x)$ does not give any contribution to the probability of failure. The upper tail of the truncated strength distribution contributes to the probability of failure depending on its relative interaction with the upper tail of the load distribution. Since the interaction between load and strength distribution is of a general form, as shown in Fig. 1, the upper tail contribution $F_R(x)$ to the probability of failure diminishes very quickly with increasing distance from the mean strength. Consequently, the greatest contribution of the strength density function to the probability of failure during service stems from the region close to the proof-load test level (Fig. 1). Since the determination of the probability of failure with

certain confidence requires knowledge of the distribution functions of the load and of the truncated strength R_0, it can be inferred that the required cost of coupon tests to enable the determination of the probability of failure with certain confidence is strongly dependent on the proof-load level. This cost will be called coupon testing cost or material characterization cost. If different structural subsystems are used with differing materials, the total coupon testing cost is the sum of the characterization costs for each material.

The expected cost due to proof testing is the statistically expected cost of structural testing in which one structure after another is tested at a certain proof-load level, until a structure is obtained that passes the applied proof load. This cost includes the cost of the structures after their completion plus the actual cost of proof testing. As Eq. (31) clearly indicates, this structural qualification cost is also strongly dependent on the proof-load test level. It should be recalled that the term structure refers here to structural subsystems such as struts, pressure vessels, etc., and that the structural system, such as a spacecraft structure, may consist of more than one subsystem. If a number of structural subsystems require qualification, then the total proof testing cost is the sum of the statistically expected costs due to proof testing for each subsystem.

From a structural utilization point of view, it is not only important to consider the costs of coupon testing and proof testing, but also the cost that will be incurred if the structure fails during the time of its use. In space applications, this cost may range from cost of total mission loss to negligibly small cost, depending on whether structural failure occurs at the beginning of a mission or after the mission objectives have been fulfilled. This cost would also depend on whether structural failure causes complete destruction or only some mission degradation. The statistically expected value of this cost, which will be called mission degradation cost, is the product of the actual cost of mission degradation and the probability of occurrence of this degradation, which is the probability of structural failure.

The preceding discussion indicates that the total statistically expected cost EC for n structural subsystems is the sum of the statistically expected costs EC_i for each ith structural subsystem, which can be written as

$$EC = \sum_{i=1}^{n} EC_i \qquad (38a)$$

$$EC_i = C_i(\epsilon_i) + q_i(\epsilon_i)C_{0i} + p_{fi}(\epsilon_i, \nu_i)C_f \qquad (38b)$$

where the three terms on the right side of Eq. (38b) represent coupon testing cost, proof testing cost, and mission degradation cost, respectively, of the ith subsystem. The proof test level ϵ_i for the ith structural subsystem is the ratio of the proof load S_{0i} to the mean structural strength $\bar{R}_i$; C_i is the coupon testing cost for the ith structural subsystem; q_i is the expected number of the ith structural subsystem failing before the one surviving the proof load is obtained; C_{0i} is the cost of losing one of the ith structural subsystem during proof load; C_f is the actual cost of mission degradation; p_{fi} is the probability of structural failure of the ith structural subsystem during the mission. The approximation of the summation sign for the mission degradation cost in Eq. (38) is on the conservative side (Refs. 2 and 3). It follows from the developments in the previous section, that p_{fi} is not only a function of ϵ_i but also of the central safety factor, $\nu_i = \bar{R}_i / \bar{S}_i$, which is the ratio of mean strength $\bar{R}_i$ to mean load $\bar{S}_i$, or of some other central measure of location. It should be noted that ν_i is numerically different from the conventional safety factor, which is usually based on percentiles of R_i and S_i, but plays, in principle, the same role.

The equations in Section V are valid for any ith structural subsystem. Since $S_{0i} = \epsilon_i \bar{R}_i$, the probability of failure p_{0i} of the ith structural subsystem due to the proof load S_{0i} given by Eq. (31) can be expressed in terms of ϵ_i. It can be shown that

$$q_i(\epsilon_i) = \frac{p_{0i}(\epsilon_i)}{1 - p_{0i}(\epsilon_i)} \qquad (39)$$

which gives the functional dependence of q_i on ϵ_i.

The coupon testing cost requires some explanation. Note that it is the subsystem that is subjected to proof testing. For this reason, the original subsystem strength R_i is truncated into R_{0i}. Since the distribution of R_i and hence the distribution of R_{0i} are derived from the distribution of the coupon strength R_{ci} for the ith subsystem (i.e., Eq. (11), and since only the strength distribution function associated with the strength value $R_i \geq S_{0i}$ (i.e., R_{0i}), is needed in evaluating the probability of failure, it is necessary to establish the coupon strength distribution, with certain statistical confidence, only for those coupon strength values $R_{ci} > S_{ci}$ with S_{ci} being the value associated with the truncation point S_{0i} (or proof load) of the subsystem strength. Let $\bar{\epsilon}_i$ be the ratio of S_{ci} to the mean coupon strength $\bar{R}_{ci}$ for the ith subsystem; i.e., $\bar{\epsilon}_i = S_{ci}/\bar{R}_{ci}$. The functional dependence of C_i on $\bar{\epsilon}_i$ should be such that C_i is increasing with increasing absolute difference between $\bar{\epsilon}_i$ and 1, i.e., with $|\bar{\epsilon}_i - 1|$ (see Ref. 3 for a detailed discussion). Thus $\bar{\epsilon}_i$ should be expressible as a function of ϵ_i so that C_i in Eq. (38) can be written as a function of ϵ_i. In this report, the following assumptions are made: (1) in the Weibull distribution, the parameter x_0 is equal to zero, and (2) in Eq. (16b), for each ith structural subsystem the expression $(\phi_1 + \phi_2)$ is independent of the space coordinates. While the first assumption is not particularly restrictive, the second assumption implies a homogeneous stress field within each structural subsystem. With these two assumptions, and using Eqs. (11) and (16b), it can be easily shown that $\bar{\epsilon}_i = \epsilon_i$.

It is now assumed that the coupon testing cost for the ith structural subsystem can be approximated by an expression of the following form (Ref. 3):

$$C_i(\epsilon_i) = A_i + \delta_i B_i \left| \epsilon_i - 1 \right|^{m_i} \tag{40}$$

where A_i is the minimum cost of coupon tests necessary for the determination of the mean value of coupon strength with certain confidence. The terms B_i and m_i are constants, and δ_i is a constant that may take different values δ_i^+ and δ_i^- for $\epsilon_i > 1$ and $\epsilon_i < 1$, respectively.

If $\epsilon_i < 1$, the significant part of the truncated strength distribution for the evaluation of the probability of failure is located between the proof-load level and the central portion of the strength distribution, whereas, if $\epsilon_i > 1$, the significant part lies beyond the central portion of the distribution. To establish the strength distribution with certain confidence, this suggests that a larger sample of coupons is required if $\epsilon_i > 1$ as compared to $\epsilon_i < 1$ for the same value $|\epsilon_i - 1|$.

When one considers the preceding remarks and divides Eq. (38) by C_f, the total relative expected cost $EC^* = EC/C_f$ and the relative expected cost for the ith subsystem $EC_i^* = EC_i/C_f$, become

$$EC^* = \sum_{i=1}^{n} EC_i^* \tag{41a}$$

$$EC_i^* = \alpha_i + \delta_i \beta_i \left| \epsilon_i - 1 \right|^{m_i} + q_i(\epsilon_i)\gamma_i + p_{fi}(\epsilon_i, \nu_i) \tag{41b}$$

where $\alpha_i = A_i/C_f$, $\beta_i = B_i/C_f$ and $\gamma_i = C_{0i}/C_f$. Note that β_i and γ_i indicate the relative importance of the ith subsystem with respect to the actual cost of mission degradation if the ith subsystem fails and, as will be shown later, these values are the important parameters in the optimization process.

The optimization problem can now be stated as either one of minimizing the structural weight subject to a constraint on the relative expected cost given in Eq. (41), or one of minimizing the relative expected cost EC^* subject to a constraint on the structural weight. Both approaches are essentially the same. In this report, the optimization problem is stated as follows:

Minimize the total structural weight G subject to the maximum expected cost constraint $EC^* \leq EC_a^*$.

The objective function

$$G = \sum_{i=1}^{n} G_i$$

with G_i being the ith subsystem weight, can be written as a linear function of the design variables h_i (i=1, 2, $\cdots$, n), where h_i may, e.g., represent the cross-sectional area of the ith subsystem strut or the thickness of the ith subsystem pressure vessel; thus

$$G = \sum_{i=1}^{n} g_i h_i \qquad (42)$$

where g_i represents functions of physical and geometrical parameters of the ith subsystem.

It is emphasized that if the proof-load test is not performed or is not considered (i.e., if all $q_i(\epsilon_i) = 0$), and if the material properties are well known to engineers so that coupon tests are not needed (i.e., if all $\alpha_i = \beta_i = 0$), then the maximum constraint EC_a^* becomes the maximum constraint of the probability of failure, and the problem reduces the optimum design based on a reliability constraint criteria that is discussed in Refs. 16-21.

Since Eq. (41) is the only constraint, and since the objective function is linear in h_i, the constraint is always active; i.e., at optimum, the

equality sign should hold in the constraint. Note that the central safety factor ν_i in Eq. (41) can be expressed as a function of h_j, j=1, 2, $\cdots$, n; i.e., $\nu_i = \nu_i (h_1, h_2, \cdots, h_n)$. Using the method of Lagrangian multipliers, one can show that at optimum the following equations hold:

$$\frac{\partial EC_i^*}{\partial \epsilon_i} = 0, \qquad i = 1, 2, \ldots, n \qquad (43a)$$

$$EC^* = EC_a^* \qquad (43b)$$

Equation (43) states that for an optimum structural weight, the proof-load level ϵ_i to be applied to the ith structural subsystem should also be optimum in the sense that corresponding to a given safety factor ν_i the relative expected cost should be minimum at that level.

As for the optimization technique, depending on whether the structural system is statically determinate or statically indeterminate, the iterative procedure or the gradient move method can be employed, respectively. This subject is discussed in detail in Ref. 2.

VII. NUMERICAL EXAMPLE

A 20-in.-diam spherical pressure vessel is to be designed to sustain an internal pressure S_s after proof testing for 360 h. The weight of the vessel is to be minimized for an appropriate choice of proof-load level ϵ (or S_0) and vessel wall thickness h in such a way that the total relative expected cost EC^* does not exceed a certain assigned value EC_a^* (constraint). The sustained pressure is assumed to be normally distributed with mean value $\bar{S}_s$ = 1000 psi and 2% coefficient of variation. (Since only one subsystem is considered, the subscript i is dropped.) It is assumed that the material is titanium Ti-61A-4V and that the coupon strength has a Weibull distribution with a mean value of $\bar{R}_c$ = 160,000 psi and coefficient of variation of 10%, with a coupon size of 8 in. long, 1/2 in. wide and 1/4 in. thick. Based on the discussion in Section VI, it is further assumed that in Eq. (40), $\delta^- = 1$ for $\epsilon < 1$ and $\delta^+ = 2$ for $\epsilon > 1$, and m = 1. The vessel is to be designed for room temperature at which the parametric values in Eq. (24) for U(t) are b = 0.5, r = 0.5 and τ = 0.713. The stress field is assumed to be such that $\phi_1 = \phi_2 = \phi$ = constant.

The Weibull distribution for the coupon strength is given in Eq. (11), from which, it follows that

$$\sigma_{R_c} = \frac{\left[\Gamma\left(1 + \frac{2}{k}\right) - \Gamma^2\left(1 + \frac{1}{k}\right)\right]^{1/2}}{\Gamma\left(1 + \frac{1}{k}\right)} \quad (44)$$

and

$$\bar{R}_c = \frac{x_0}{\left(\frac{V_c}{v}\right)^{1/k}} \Gamma\left(1 + \frac{1}{k}\right) \quad (45)$$

where σ_{R_c} is the coefficient of variation of the coupon strength equal to 0.1, and $\bar{R}_c$ is the mean coupon strength equal to 160,000 psi. Hence, the parameter k can be evaluated from Eq. (44), and then x_0 can be computed from Eq. (45).

In accordance with the discussion in the previous sections,

$$\bar{R} = \frac{x_0}{2\phi\left(\frac{V}{v}\right)^{1/k}} \Gamma\left(1 + \frac{1}{k}\right) \quad (46)$$

$$\phi = \frac{d}{4h} \quad (47)$$

$$v = \frac{\bar{R}}{\bar{S}_s} \quad (48)$$

$$h = \left\{ \frac{v\bar{S}_s d\left(\pi d^2\right)^{1/k}}{2x_0 \Gamma\left(1 + \frac{1}{k}\right)} \right\}^{k/(k-1)} \tag{49}$$

$$q(\epsilon) = \frac{p_0(\epsilon)}{1 - p_0(\epsilon)} = \exp\left\{ \left[\epsilon \, \Gamma\left(1 + \frac{1}{k}\right) \right]^k \right\} - 1 \tag{50}$$

in which the daimeter of the vessel d = 20 in., the vessel material volume $V = \pi d^2 h$, and the proof load level $\epsilon = S_0/\bar{R}$ with S_0 being the proof load.

According to Eq. (37), the probability of vessel failure due to S_s, after the vessel passed the proof test, can be written as

$$p_f = \frac{1}{(2\pi)^{1/2} \sigma_s \bar{S}_s} \int_{S_0 U(T)}^{\infty} \exp\left[-\frac{1}{2}\left(\frac{x - \bar{S}_s}{\bar{S}_s \sigma_s}\right)^2 \right] \left(1 - \exp\left\{ -\left[\frac{x\Gamma\left(1 + \frac{1}{k}\right)}{U(T)\bar{R}} \right]^k + \left[\frac{S_0 \Gamma\left(1 + \frac{1}{k}\right)}{\bar{R}} \right]^k \right\} \right) dx \tag{51}$$

where $\sigma_s = 0.02$ is the coefficient of variation of S_s and where $p_s = p_f$.

The introduction of the transformation $y = x/\bar{R}$ into Eq. (51) yields

$$p_f = \frac{1}{(2\pi)^{1/2}} \frac{v}{\sigma_s} \int_{\epsilon U(T)}^{\infty} \exp\left\{ -\frac{1}{2}\left(\frac{yv - 1}{\sigma_s}\right)^2 \right\} \left(1 - \exp\left\{ -\left[\frac{y\Gamma\left(1 + \frac{1}{k}\right)}{U(T)} \right]^k + \left[\epsilon \, \Gamma\left(1 + \frac{1}{k}\right) \right]^k \right\} \right) dy \tag{52}$$

In this particular example, since there is only one subsystem, Eq. (41) can be written as

$$EC^* = \alpha + \delta\beta|\epsilon - 1| + q(\epsilon)\gamma + p_f(\epsilon, v) \tag{53}$$

in which the subscript i has been dropped and it can be shown that the optimum values of v and ϵ can be determined from the following two equations:

$$\frac{\partial EC^*}{\partial \epsilon} = 0 \tag{54a}$$

$$EC^* = EC_a^* \tag{54b}$$

The relative expected cost EC^* in Eq. (53) is plotted as a function of ϵ for different values of γ and β with $q(\epsilon)$ and $p_f(\epsilon, v)$ being given by Eqs. (50) and (52). These plots are shown in Fig. 11 for a particular value $v = 2.1$. The constant value α in Eq. (53) has been disregarded in these figures, since it has no effect on the optimization process. Including a nonzero value for α would give to the plots a corresponding shift parallel to the EC^* axis.

Those values of ϵ for which EC^* becomes minimum for a given v are denoted by ϵ^*. The solution space of the optimum design, Eq. (54), can then be constructed by plotting the locuses for different values of v as shown in Fig. 12. This figure is the extended version of Fig. 11, and is referred to as the optimum design space.

The optimum design procedure can now be summarized as follows:

(1) Construct the optimum design space, e.g., Fig. 12.

(2) Read ν and ϵ^* from the optimum design space constructed in step (1) for specified constraint EC_a^* and given values of γ and β.

(3) With the safety factor ν obtained in step (2), the optimum (minimum) thickness h of the vessel or the minimum weight G can be determined from Eq. (49).

If the relative expected cost EC^* is to be minimized, subject to the constraint on the vessel weight (or safety factor ν_a), the relationship of Eq. (54a) is still valid but Eq. (54b) should be replaced by $\nu = \nu_a$. Hence, the minimum relative expected cost design can be obtained either by plotting EC^* as a function of ϵ for given β, γ, and constraint ν_a, such as Fig. 11, to find ϵ^* and minimum EC^*, or by reading ϵ^* and minimum EC^* directly from the optimum design space constructed previously, for a specified constraint ν_a and given value of γ. Numerical results for three specific cases are given in Table 1.

It should be noted that if the proof-load test is not performed or not considered (i.e., if $q(\epsilon) = 0$), and if the material property is well known so that the coupon tests are not needed (i.e., if $\alpha = \beta = 0$), then the maximum constraint EC_a^* on the relative expected cost becomes the maximum constraint on the probability of failure. The problem reduces then to the optimum design based on the reliability criteria. This design is termed "Standard Optimum Design" in Table 1.

Table 1. Optimum design of pressure vessel

Parameter	$\gamma = 10^{-7}$	$\gamma = 10^{-6}$	$\gamma = 10^{-5}$	$\gamma = 10^{-4}$	Standard Optimum Design[a]
$\beta = 0.0$, $EC_a^* = 10^{-6}$					
Thickness h, in.	0.1869	0.2086	0.2472	0.300	0.6311
ϵ^*	1.11634	1.00845	0.8568	0.70928	0.0
S_0, psi	2130	2128	2113	2089	0.0
ν	1.9082	2.1104	2.4668	2.9450	5.8300
p_f	0.7934×10^{-7}	0.4787×10^{-7}	0.4223×10^{-7}	0.706×10^{-7}	10^{-6}
$\beta = 0.0$, $EC_a^* = 10^{-5}$					
Thickness h, in.	0.1746	0.1852	0.2065	0.2447	0.5134
ϵ^*	1.179	1.114	1.0091	0.850	0.0
S_0, psi	2113	2108	2110	2088	0.0
ν	1.7925	1.8926	2.091	2.444	4.8238
p_f	0.174×10^{-5}	0.177×10^{-5}	0.472×10^{-6}	0.72×10^{-6}	10^{-5}
$\beta = 0.0$, $EC_a^* = 10^{-4}$					
Thickness h, in.	0.1661	0.1727	0.1833	0.2042	0.4176
ϵ^*	1.2172	1.179	1.116	1.008	0.0
S_0, psi	2090	2094	2091	2087	0.0
ν	1.713	1.775	1.874	2.07	3.99
p_f	0.374×10^{-4}	0.2115×10^{-4}	0.1242×10^{-4}	0.5731×10^{-5}	10^{-4}
$\beta = 10^{-5}$, $EC_a^* = 10^{-5}$					
Thickness h, in.	0.1765	0.1870	0.2066	0.2484	-
ϵ^*	1.169	1.096	1.0086	0.8510	-
S_0, psi	2117	2093	2110	2089	-
ν	1.81	1.91	2.092	2.477	-
p_f	0.1042×10^{-5}	0.8236×10^{-6}	0.4639×10^{-6}	0.6941×10^{-6}	-

[a]The Standard Optimum Design is possible only when $\beta = 0$.

Table 1 (contd)

Parameter	$\gamma = 10^{-7}$	$\gamma = 10^{-6}$	$\gamma = 10^{-5}$	$\gamma = 10^{-4}$	Standard Optimum Design[a]
	$\beta = 10^{-5}$, $EC_a^* = 10^{-4}$				
Thickness h, in.	0.1665	0.1728	0.1834	0.2042	-
ϵ^*	1.2170	1.178	1.115	1.008	-
S_0, psi	2088	2092	2090	2087	-
ν	1.716	1.776	1.876	2.07	-
P_f	0.34×10^{-4}	0.1642×10^{-4}	0.1207×10^{-4}	0.573×10^{-5}	-
	$\beta = 10^{-4}$, $EC_a^* = 0.5 \times 10^{-4}$				
Thickness h, in.	0.1734	0.1807	0.1920	0.2158	-
ϵ^*	1.1865	1.138	1.073	0.9594	-
S_0, psi	2114	2104	2098	2090	-
ν	1.781	1.850	1.960	2.178	-
P_f	0.176×10^{-5}	0.349×10^{-5}	0.358×10^{-5}	0.253×10^{-5}	-
	$\beta = 10^{-4}$, $EC_a^* = 10^{-4}$				
Thickness h, in.	0.1671	0.1744	0.185	0.2042	-
ϵ^*	1.216	1.170	1.107	1.008	-
S_0, psi	2090	2094	2093	2087	-
ν	1.7218	1.791	1.891	2.070	-
P_f	0.1×10^{-4}	0.1277×10^{-4}	0.93×10^{-5}	0.574×10^{-5}	-

[a]The Standard Optimum Design is possible only when $\beta = 0$.

VIII. DISCUSSION AND CONCLUSION

Using Eq. (53), one obtains curves of the relative expected cost EC^* versus proof load level ϵ for different β, and for different safety factors ν. Figure 11 shows representative curves for four γ values, three β values, and a particular safety factor $\nu = 2.1$. In Fig. 11, the relative expected cost EC^* changes very little for ϵ less than approximately 0.85. For other safety factors, EC^* behaves similarly, indicating that there is no advantage in conducting proof testing below a certain value of ϵ. In all three cases, $\beta = 0$, $\beta = 10^{-5}$ and $\beta = 10^{-4}$, the optimum proof-load levels are in the vicinity of $\epsilon = 1.0$ with a slight and expected tendency of the optimum proof-load levels ϵ^* toward unity with increasing β. It is due to this fact that under reasonable relative expected cost constraints, the optimum proof-load level ϵ^* will fall with great likelihood within the range of two standard deviations around the mean value $\overline{R}$. From the designer's point of view, this is desirable, since in general, a considerably greater number of coupon tests is required for characterizing the truncated strength distribution with a certain level of statistical confidence if ϵ^* falls outside this region. It is noteworthy that for $\nu = 2.1$, EC^* is very sensitive to changes of ϵ in certain regions,

such as $0.9 \lesssim \epsilon \lesssim 1.0$ and $\epsilon \gtrsim 1.1$; $\epsilon \gtrsim 0.97$, EC^* is also sensitive to γ. Similar statements hold also for safety factors different from $\nu = 2.1$.

In Fig. 12, the relative expected cost EC^* is plotted as a function of the optimum proof-load level ϵ^* for the same three values of β as in Fig. 11. Figure 12 is an extension of Fig. 11 in that the lines for $\nu = 2.1$ give the optimum points indicated in Fig. 11, while the lines for the other values of ν reflect the optimum points of similar curves as those in Fig. 11.

The first set of curves for $\beta = 0$ in Fig. 12 shows that when the coupon test is not needed, the relative expected cost EC^* can be made as small as desired simply by decreasing ϵ^* and increasing the safety factor ν, or the weight which, in this case, is proportional to ν. This result is a consequence of the fact that EC^* is not, in this case, a function of the cost of coupon test. If the cost of coupon testing is considered (i.e., if $\beta \neq 0$ as for the second and third set of curves in Fig. 12), then the relative expected cost EC^* has a lower limit. This implies that in such cases a relative expected cost constraint less than this lower limit yields no feasible solution. It is evident from Fig. 12 that

for $\beta \neq 0$ the absolute optimum proof-load level is in the vicinity of $\epsilon^* = 1.0$ for $\beta = 10^{-5}$ with $\nu = 2.2$ and for $\beta = 10^{-4}$ with $\nu = 2.1$. Additional details regarding the influence of the cost of coupon tests on the optimum design are given in Ref. 3.

Table 1 gives specific numerical results for different values of β and for specified relative expected cost constraints EC_a^*. It is particularly instructive to compare the results of the Standard Optimum Design $\epsilon^* = 0$ with those of the optimum design considering the proof-load test; i.e., for $\gamma = 10^{-7}$ to 10^{-4}. Not only is considerable weight saving realized (weight is proportional to h), but also a great reduction of the probability of failure p_f is obtained if the proof-load level is considered as a design variable. The percentage of weight saving of the optimum design with proof-load tests as compared to the design without proof-load tests is much higher in this case than in the examples given in Refs. 2 and 3. This is because in the present case, the coefficient of variation of the strength R of the vessel ($\sigma_R = 10\%$) is higher than the coefficient of variation of loading ($\sigma_s = 2\%$) so that the probability of failure comes mainly from the lower portion of the strength distribution, which is truncated by the proof-load. In Refs. 2 and 3, low-dispersion material ($\sigma_R = 5\%$) is used for high-dispersion loading ($\sigma_s = 20\%$). The fact that the proof-load test improves the statistical confidence of the reliability estimate is discussed in Refs. 2 and 3.

As in Refs. 2 and 3, the conclusion can be drawn here that the weight saving of the optimum design depends to a large degree on the parameter value γ. For low values of γ, one can afford to lose more vessels during proof-load testing; i.e., higher values of ϵ can be applied and these result in higher strength vessels and the saving of structural weight. This follows from Fig. 12 and Table 1.

A general conclusion that can be drawn from the preceding discussion is that in proof testing structural subsystems it is to be expected that some of these subsystems will be lost. In fact, in many cases where $\epsilon \approx 1.0$, it should be expected that approximately half of these subsystems will be destroyed during proof testing for the achievement of minimum expected cost EC^*. This is

often incompatible with prevalent thinking during project applications, particularly if the subsystems are pressure vessels. It is often expected that no pressure vessel will be destroyed during proof testing and that pressure vessels are designed to fulfill that expectation. This implies that pressure vessels are designed for the proof load rather than the expected mission environment and are proof tested at a level ϵ that corresponds to the nearly horizontal portion of the curves for EC^* in Fig. 11. As stated above, proof loads at such levels have no advantage in terms of expected cost.

In the development of this report, various simplifying assumptions were made that could be relaxed in a more extensive study. Nevertheless, it is believed that the results of this report are representative and would not undergo major qualitative changes if these assumptions were relaxed, although quantitative changes would be expected. These major assumptions and some of their implications are discussed below.

The first specific assumptions were that (1) the statistical variation of the material strength is only due to the flaw size parameter $a_j = (a/Q)_j$ in Eq. (3), and (2) it is sufficiently accurate to use the mean value of 45° for the flaw orientation so that the computational effort involved becomes tractable. The first assumption is not important in the present development because the results derived here are based on experimentally determined statistical distributions of material strength by coupon tests rather than a determination of the strength based on the statistical distribution of flaw size. The second assumption, which implies that failure occurs when the sum of the two principal stresses exceeds a critical value (Eq. 16), is considered a reasonable first approximation for cases in which both principal stresses are tensile stresses, as in thin pressure vessels. It is believed, however, that this assumption warrants additional extensive investigations based on Eq. (14) with the objective of determining, for various combinations of principal stresses, the effect of the distribution of flaw orientation on the strength distribution $F_R(S)$.

Another assumption is that strength deterioration due to time effects, i.e., due to cyclic loading and sustained loading, can be represented

by equations with deterministic parameters as shown in Section IV. This assumption can only be accepted in a qualitative fashion, since it is known from experience that the time-to-failure of a specimen has a considerable statistical variation even if the initial flaw size is the same from test to test. Considerable additional investigations, both experimental and analytical, are required before this problem can be adequately understood; perhaps it must be assumed that the parameters involved in Eqs. (20) and (21) are statistical variables.

In Section VI, the assumption that $x_\mu = 0$ in the Weibull distribution is equivalent to saying that there is no stress threshold value below which no failures occur. It is expected that this assumption has little effect on the results of the present investigations, since the proof load eliminates the lower end of the strength distribution.

Equation (38) represents the statistically expected cost that is used in the optimization process as a constraint. In this process, it is implied that the cost has a statistical distribution, which is not considered in this report. If the cost constraint is stated so that the probability of exceeding a given cost level is required to remain less than a certain value, it is necessary to also consider the statistical distribution of the cost. This aspect of the problem has not yet been treated in the literature.

A further assumption in this report (not explicitly stated) is that the mission load statistical distribution is independent of time, although the most important problems deal with dynamic loads and wide time changes of the environments, such as temperature fluctuations, radiation, etc. It is expected that the investigation in this report is only quantitatively influenced by these environmental changes while, qualitatively, the results are still valid.

The objective function in this report is the weight of the structural system. Other objective functions can be chosen, of course; for instance, the expected cost, or the reliability, can be used as an objective function that is to be minimized or maximized. For electronic systems, in which the subsystems are the electronic components or the integrated circuits that are proof tested before use, weight is usually not the critical quantity to be minimized. In such cases, cost or reliability would be more appropriately extremized.

REFERENCES

1. Barnett, R. L., and Hermann, P. C., "Proof Testing in Design with Brittle Materials," J. Spacecraft Rockets, Vol. 2, No. 6, pp. 956-961, Dec. 1965.

2. Shinozuka, M., and Yang, J. -N., "Optimum Structural Design Based on Reliability and Proof-Load Test," in Annals of Assurance Science, Proceedings of Eighth Reliability and Maintainability Conference, Vol. 8, pp. 375-391, 1969.

3. Shinozuka, M., Yang, J. -N., and Heer, E., "Optimum Structural Design Based on Reliability Analysis," in Proceedings of the Eighth International Symposium on Space Technology and Sciences, pp. 245-258, Tokyo, Japan, Aug. 1969.

4. Heer, E., and Yang, J. -N., "Optimum Pressure Vessel Design Based on Fracture Mechanics and Reliability Criteria," in Proceedings of ASCE-EMD Specialty Conference on Probabilistic Concepts and Methods in Engineering, pp. 102-106, Purdue University, Nov. 1969.

5. Foreudenthal, A. M., "Statistical Approach to Brittle Fracture," in Fracture: Volume II.

Edited by H. Liebowitz. Academic Press Inc., New York, 1968.

6. Irwin, G. R., "Fracture," Encyclopedia of Physics, Vol. 6, pp. 551-509, 1958.

7. Griffith, A. A., "The Phenomena of Rupture and Flow in Solids," Phil. Trans., Vol. 221, pp. 163-198, 1920.

8. Irwin, G. R., "Crack-Extension Force for a Part-Through Crack in a Plate," J. Appl. Mech. Vol. 84E, No. 4, pp. 651-654, Dec. 1962.

9. Tiffany, C. F., Masters, J. N., and Pall, F. A., "Some Fracture Considerations in the Design and Analysis of Spacecraft Pressure Vessels," paper given at 1966 National Metal Congress, Chicago, Ill., Oct. 1966. Published through American Society for Metals Report System as ASM Technical Report C6-2.3.

10. Brown, W. F., and Srawley, J. E., "Plane Strain Crack Toughness Testing of High Strength Metallic Materials, ASTM Special Technical Publication No. 410, American Society for Testing and Materials, Philadelphia, Pa., 1967.

11. Weibull, W., "A Statistical Theory of the Strength of Material," *Ing. Vetenskaps Akad. Handl.*, 151, Stockholm, 1939.

12. Weibull, W., "The Phenomenon of Rupture in Solids," *Ing. Vetenskaps Akad. Handl.*, 153, Stockholm, 1939.

13. Weibull, W., "A Statistical Representation of Fatigue Failures of Solids," *Kungl. Tekniska Högskolans Handl.*, 27, 1949.

14. Weibull, W., "A Statistical Distribution Function of Wide Applicability," *J. Appl. Mech.*, pp. 293-297, Sept. 1951.

15. Gumbel, E. J., *Statistical Theory of Extreme Values and Some Practical Applications, National Bureau of Standards*, Applied Mathematics Series 33, Feb. 1954.

16. Hilton, J., and Feigen, M., "Minimum Weight Analysis Based on Structural Reliability," *J. Aerosp. Sci.*, Vol. 27, pp. 641-652, 1960.

17. Kalaba, R., "Design of Minimal-Weight Structures for Given Reliability and Cost," *J. Aerosp. Sci.*, pp. 355-356, Mar. 1962.

18. Switzky, H., "Minimum Weight Design with Structural Reliability," in *AIAA 5th Annual Structures and Materials Conference*, pp. 316-322, New York, 1964.

19. Broding, W. C., Diederich, F. W., and Parker, P. S., "Structural Optimization and Design Based on a Reliability Design Criterion," *J. Spacecraft Rockets*, Vol. 1, No. 1, pp. 56-61, Jan. 1964.

20. Murthy, P. N., and Subramanian, G., "Minimum Weight Analysis Based on Structural Reliability," *AIAA J.*, Vol. 6, No. 10, pp. 2037-2038, Oct. 1968.

21. Moses, F., and Kimser, D. E., "Optimum Structural Design and Failure Probability Constraints," *AIAA J.*, Vol. 5, No. 6, pp. 1152-1158, Jan. 1967.
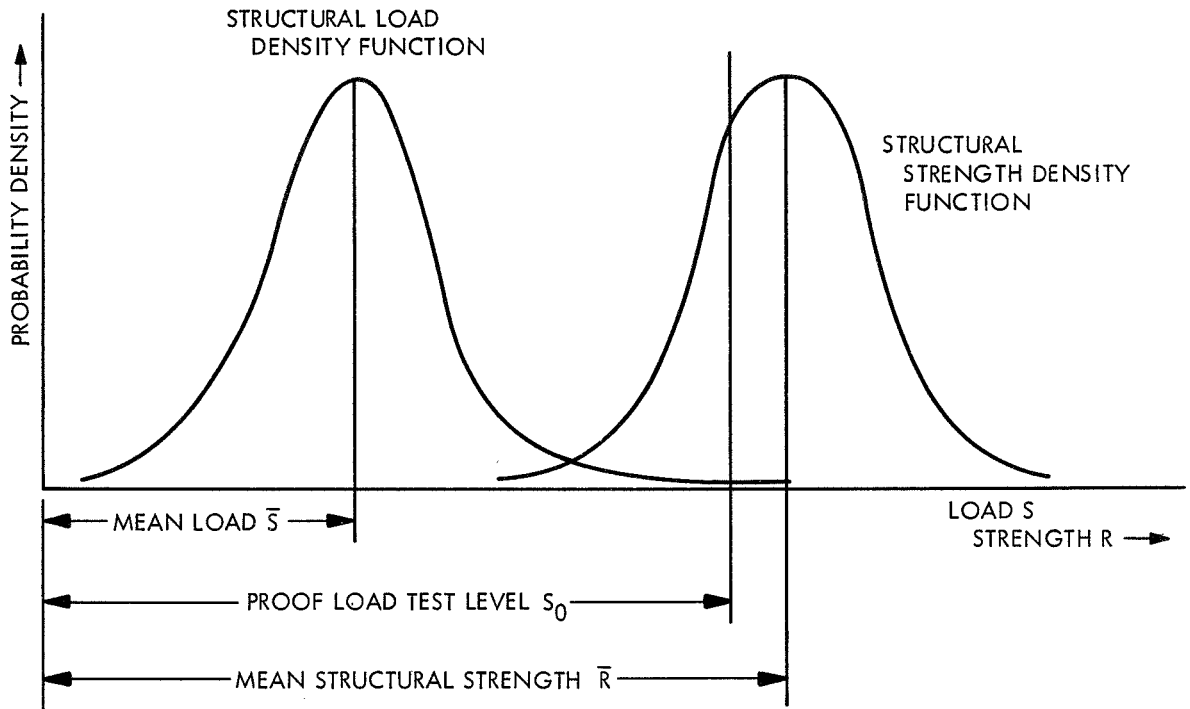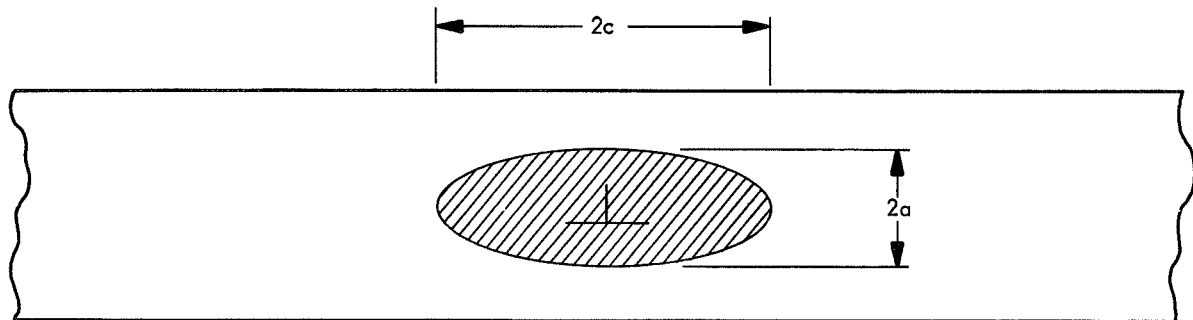
Fig. 1. Typical load and strength distributions
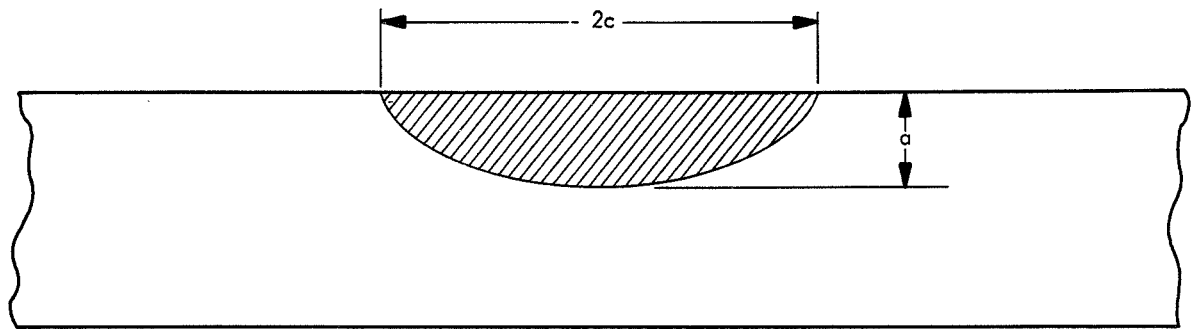
(a) $\left(\dfrac{a}{Q}\right)_{cr} = \dfrac{0.83}{\pi M_k^2} \left(\dfrac{K_{Ic}}{R}\right)^2$

(b) $\left(\dfrac{a}{Q}\right)_{cr} = \dfrac{1}{\pi M_k^2} \left(\dfrac{K_{Ic}}{R}\right)^2$

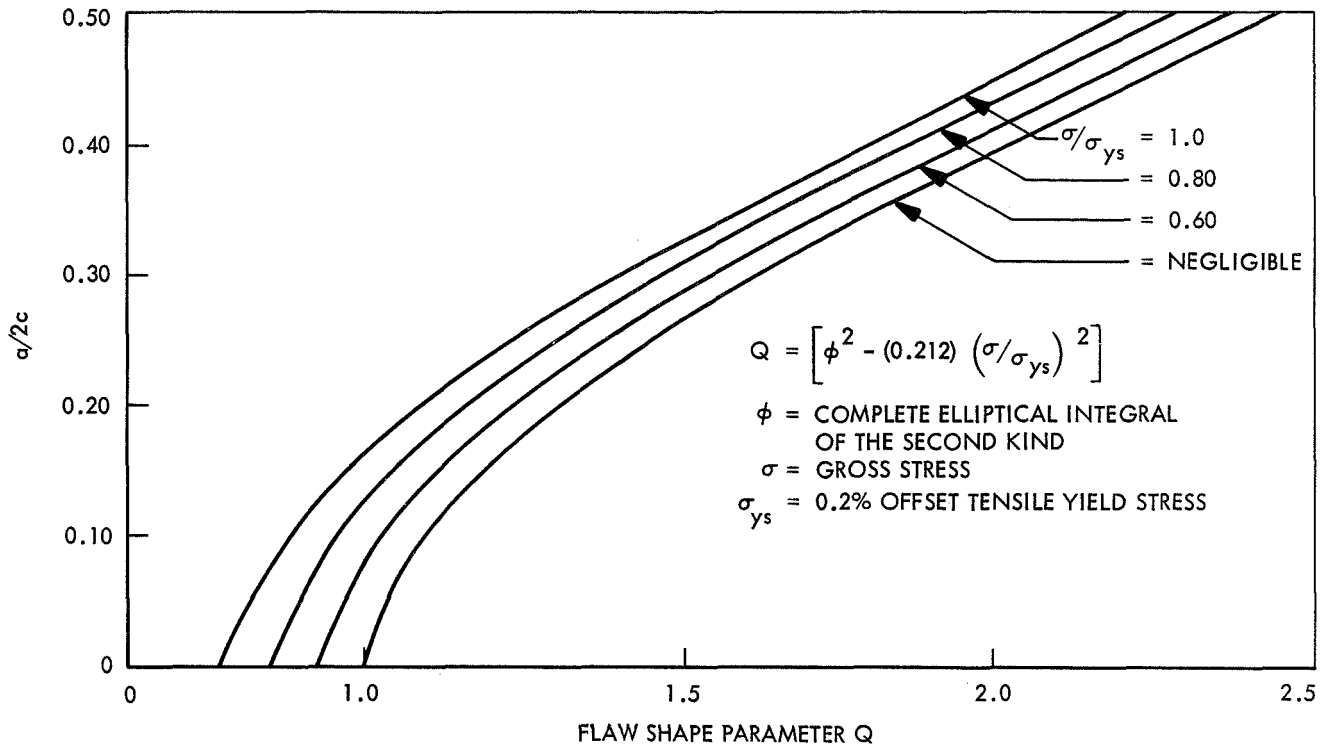Fig. 2. Elliptically shaped flaws: (a) surface flaw; (b) embedded flaw

$$Q = \left[\phi^2 - (0.212) \left(\sigma/\sigma_{ys} \right)^2 \right]$$

ϕ = COMPLETE ELLIPTICAL INTEGRAL OF THE SECOND KIND
σ = GROSS STRESS
σ_{ys} = 0.2% OFFSET TENSILE YIELD STRESS

Fig. 3. Flaw shape parameter curves for surface and internal flaws
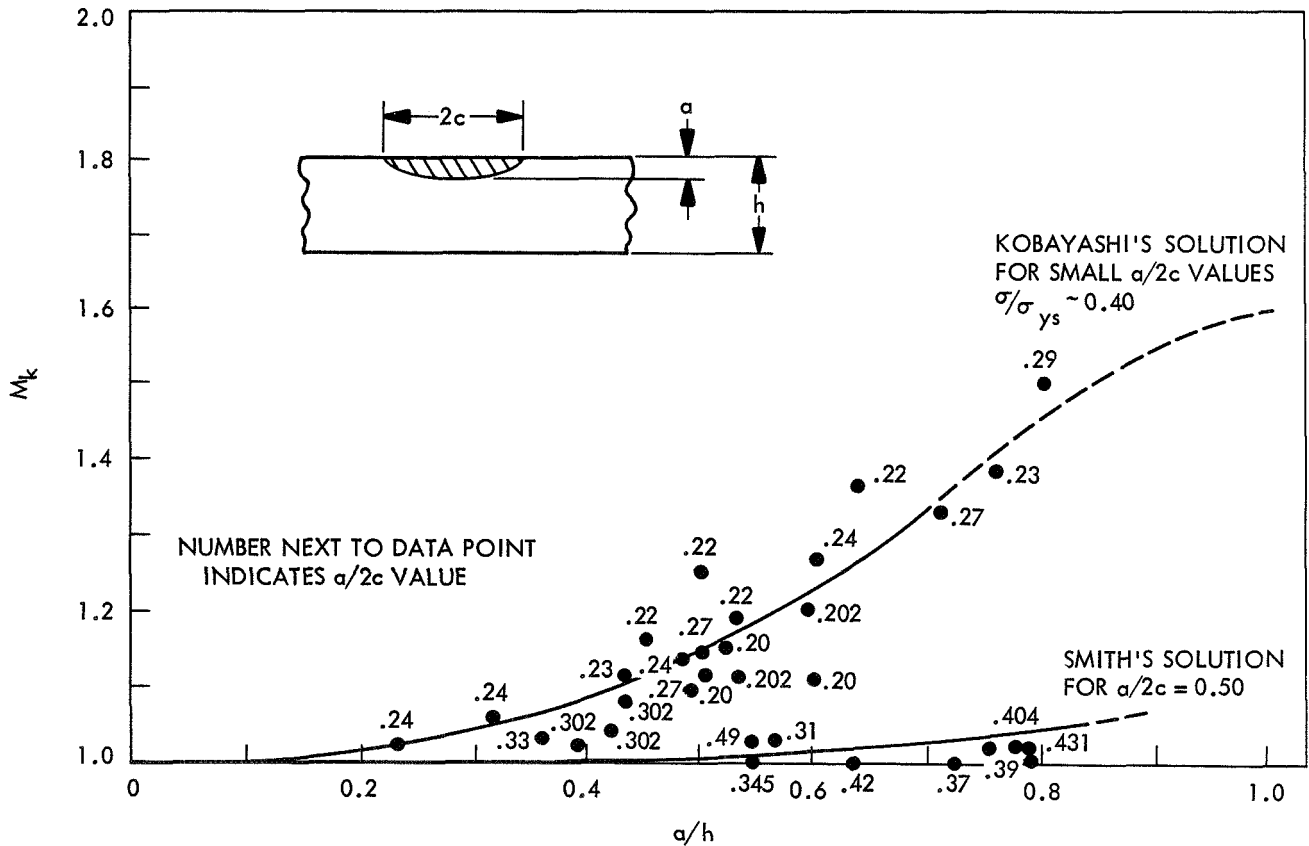
Fig. 4. Stress intensity magnification factors for deep surface flaws
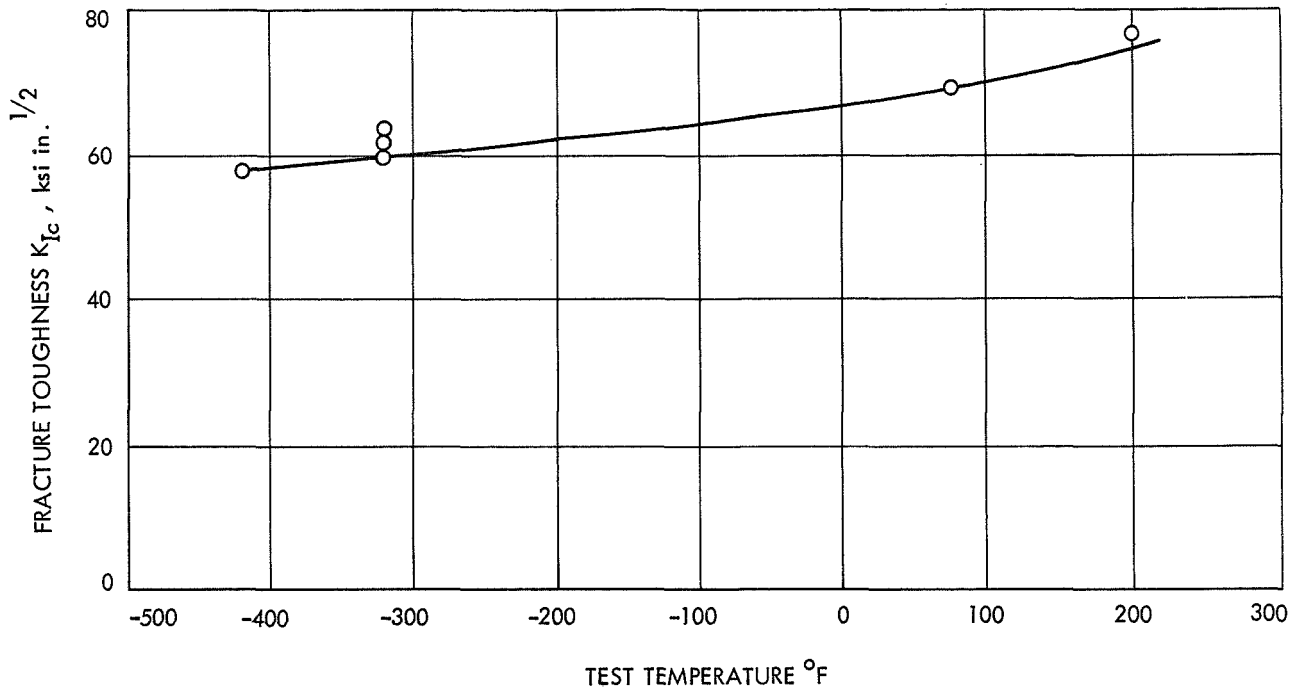
Fig. 5. Fracture toughness of annealed 6Al-4V titanium plate
at various test temperatures
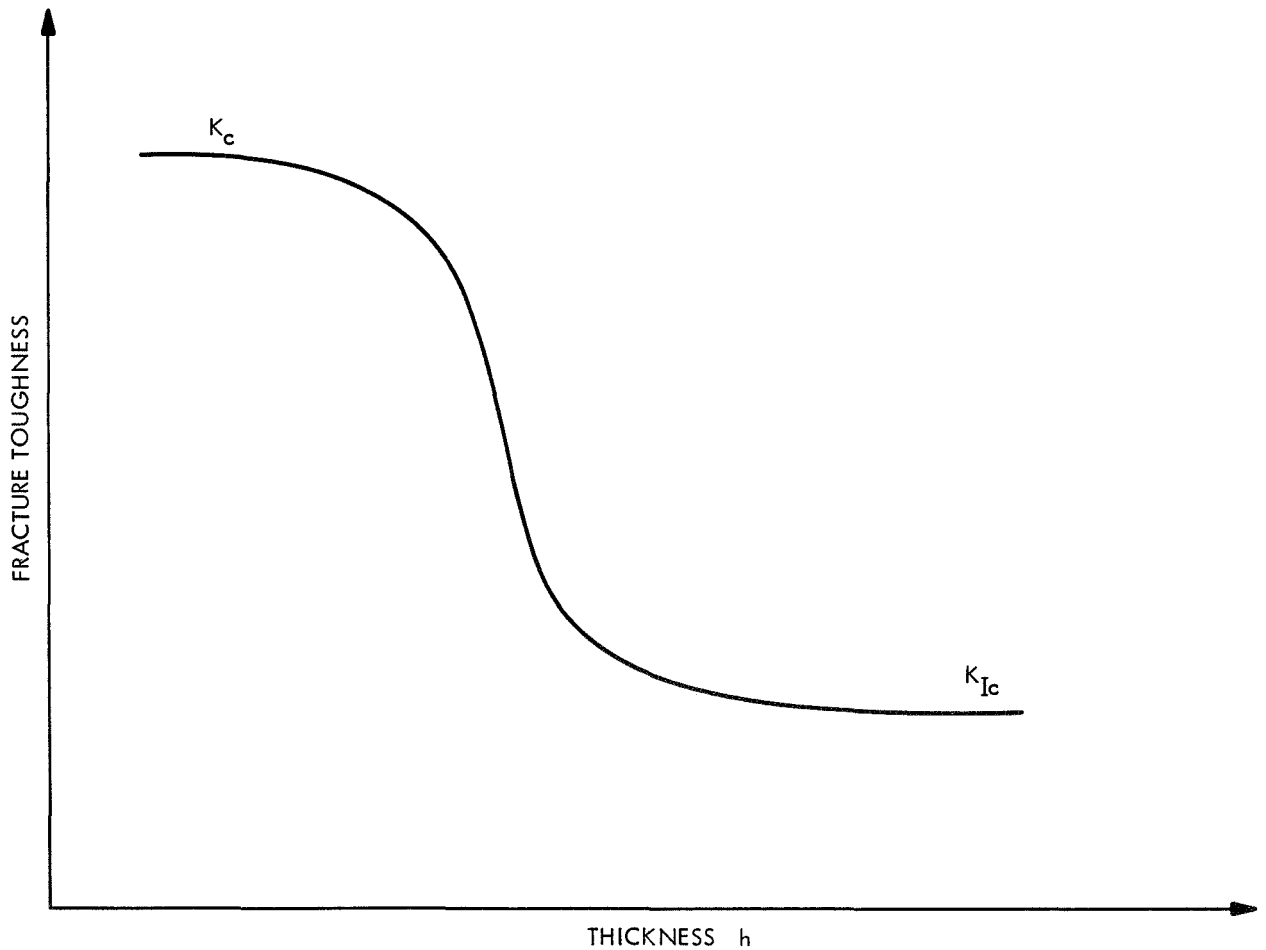
Fig. 6. Fracture toughness variation with material thickness
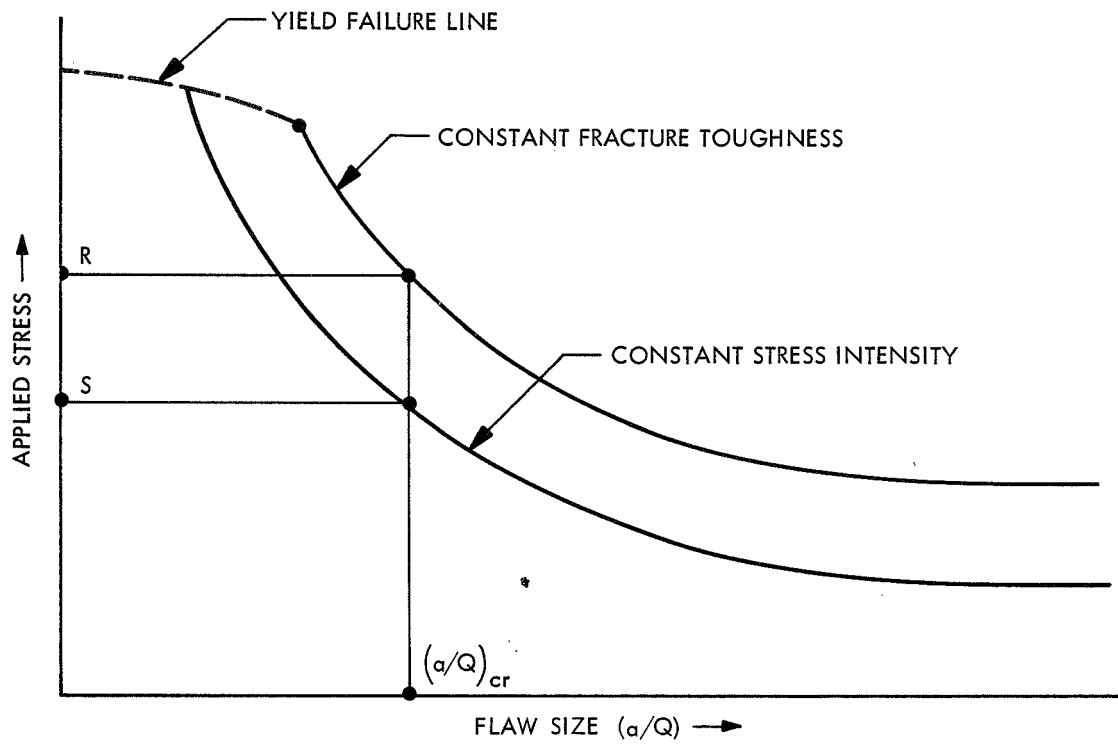
Fig. 7. Applied stress vs flaw size, for plane strain
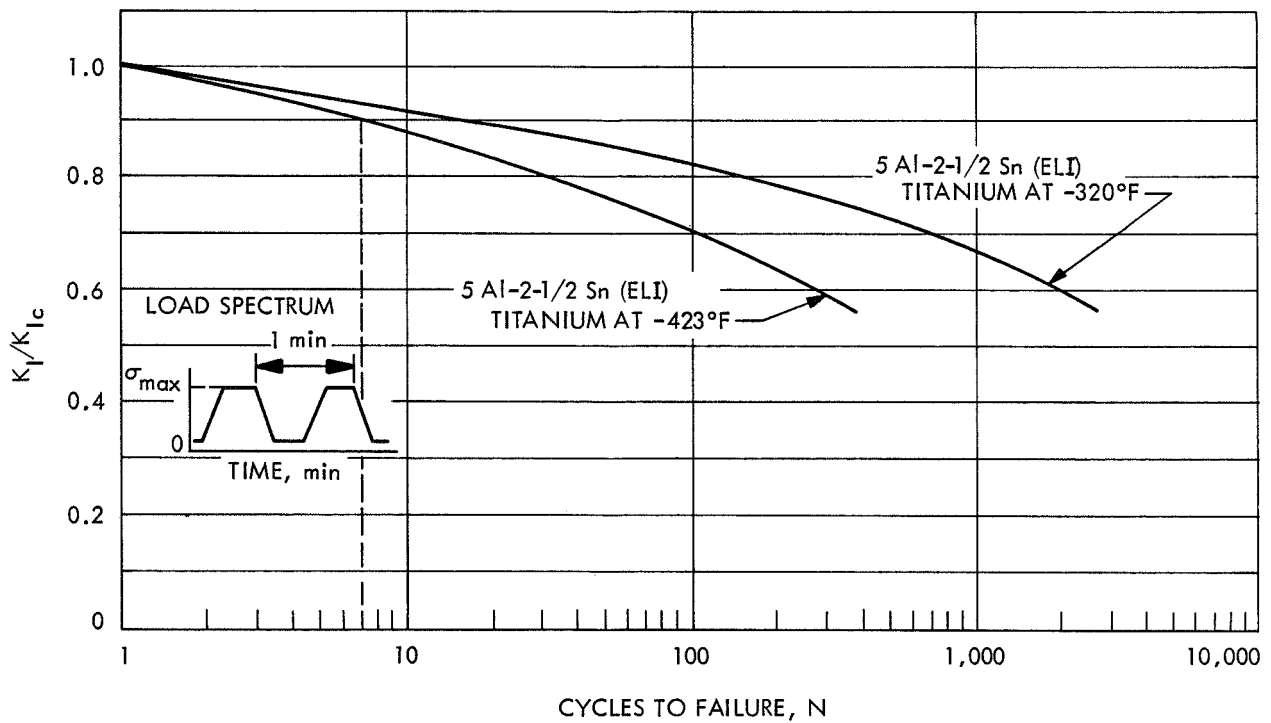
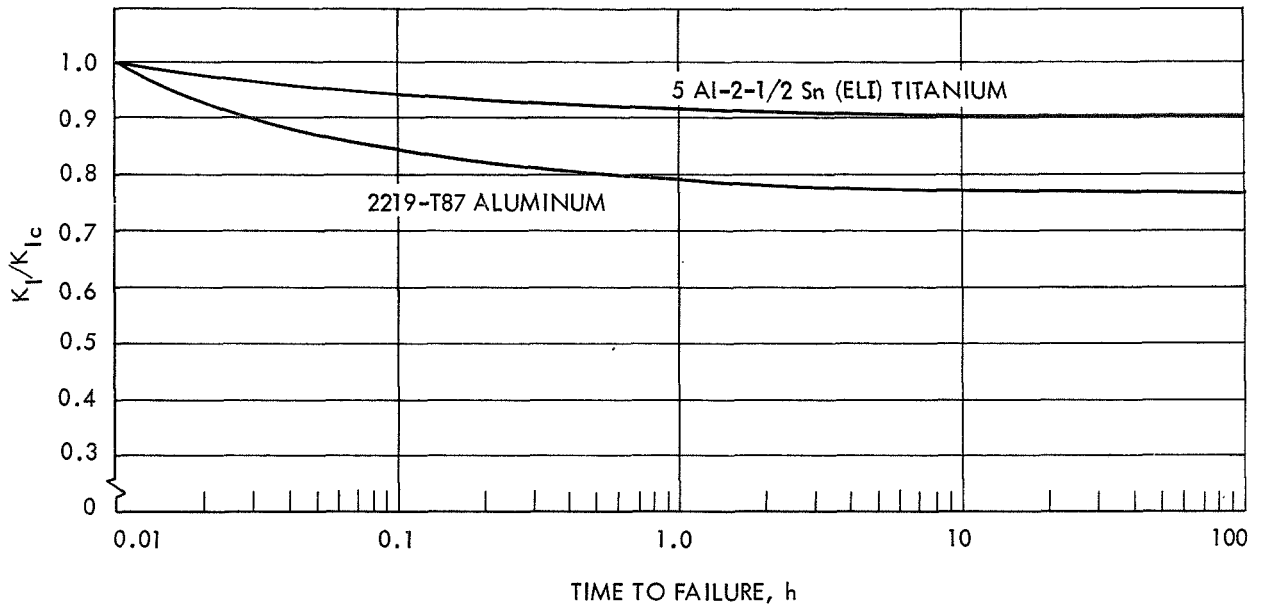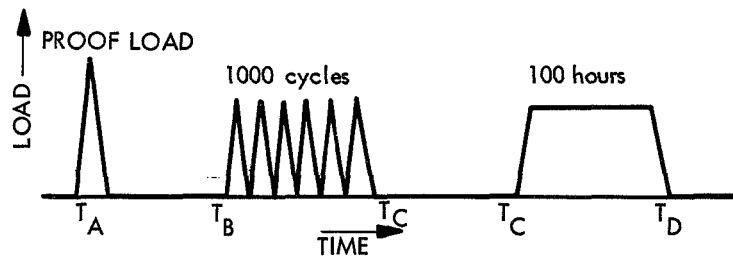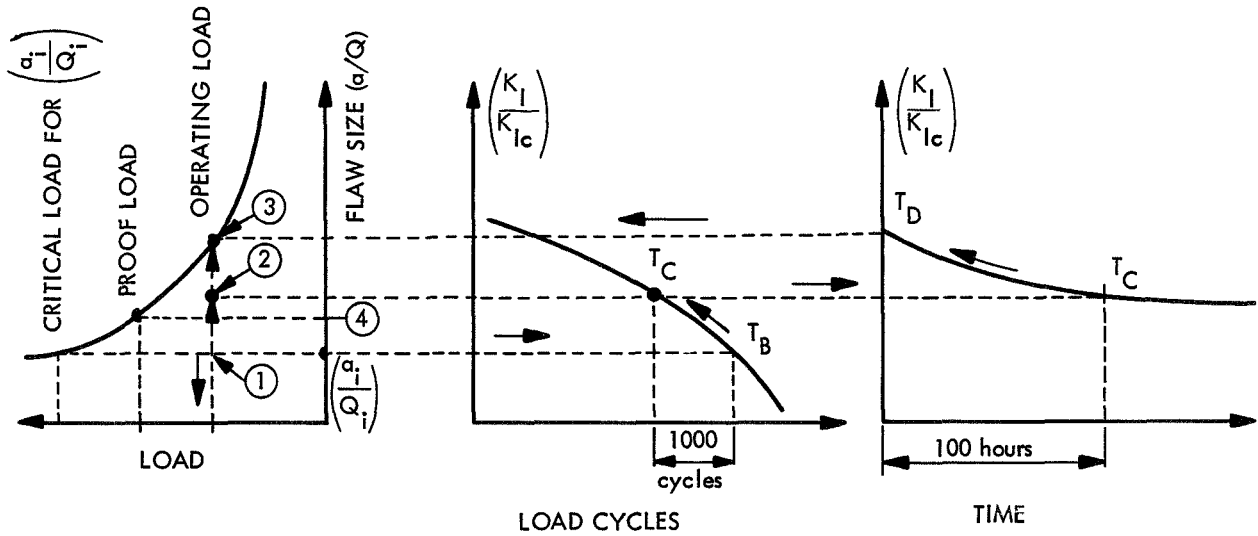Fig. 8. Operational life curves, lower bound, cyclic load

Fig. 9. Operational life curves, lower bound, sustained load

(a). TYPICAL LOAD HISTORY FOR PRESSURE VESSELS

(b). STRUCTURAL LIFE PREDICTION AND OPERATING
LOAD DETERMINATION

Fig. 10. Typical schematic design case: (a) load history for pressure vessels; structural life prediction and operating load determination
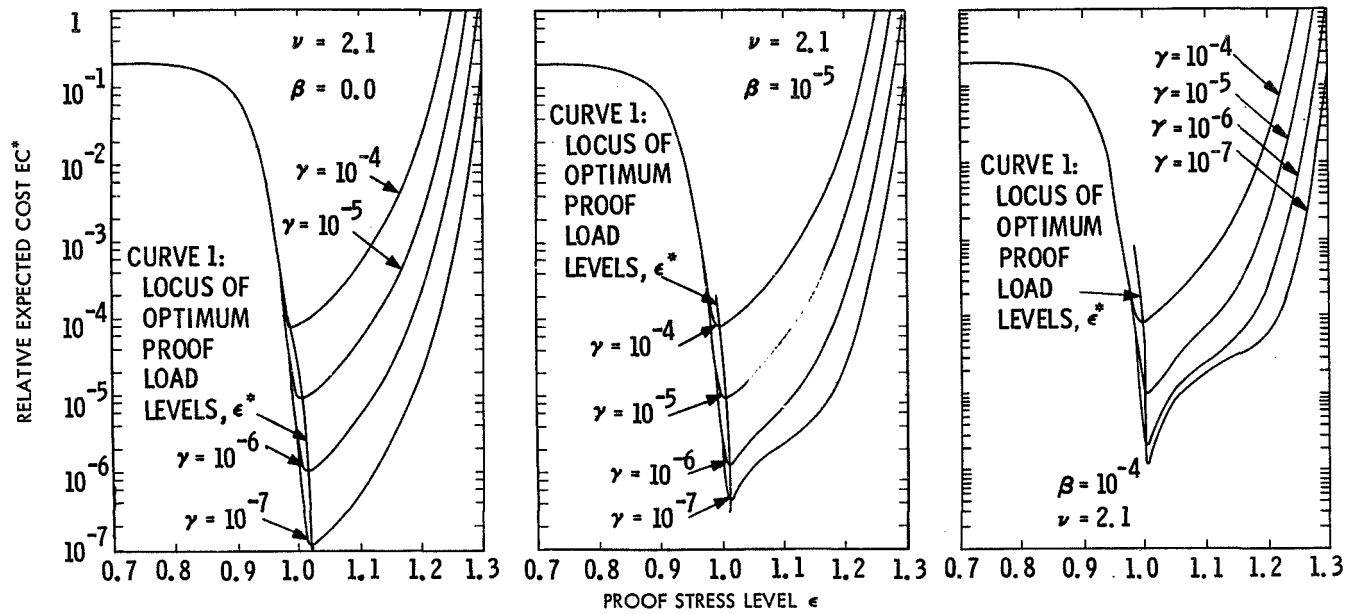
Fig. 11. Relative expected cost as a function of
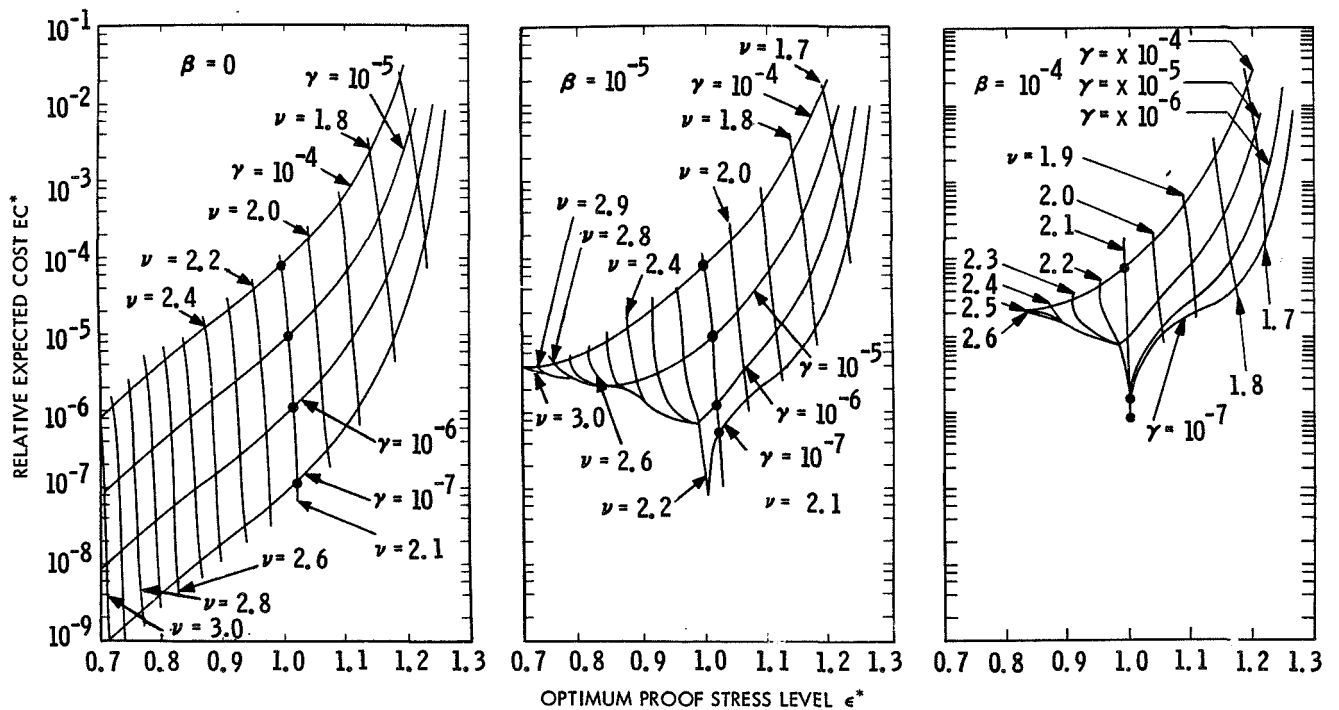proof-load level for varying values of β

Fig. 12. Relative expected cost as a function of
optimum proof-load level for varying values of β

1. Report No. 33-470	2. Government Accession No.	3. Recipient's Catalog No.

4. Title and Subtitle OPTIMUM PRESSURE VESSEL DESIGN BASED ON FRACTURE MECHANICS AND RELIABILITY CRITERIA	5. Report Date February 1, 1971
	6. Performing Organization Code

7. Author(s) Ewald Heer, Jann-Nan Yang	8. Performing Organization Report No.

9. Performing Organization Name and Address JET PROPULSION LABORATORY California Institute of Technology 4800 Oak Grove Drive Pasadena, California 91103	10. Work Unit No.
	11. Contract or Grant No. NAS 7-100
	13. Type of Report and Period Covered Technical Memorandum

12. Sponsoring Agency Name and Address NATIONAL AERONAUTICS AND SPACE ADMINISTRATION Washington, D.C. 20546	
	14. Sponsoring Agency Code

15. Supplementary Notes

16. Abstract

Spacecraft structural systems and subsystems are subjected to a number of qualification tests in which the proof loads are chosen at some level above the simulated loads expected during the space mission. Assuming fracture as a prime failure mechanism, and allowing for time effects due to cyclic and sustained loadings, this paper treats an optimization method in which the statistical variability of loads and material properties are taken into account, and in which the proof load level is used as an additional design variable. In the optimization process, the structural weight is the objective function while the total expected cost due to coupon testing for material characterization, due to failure during proof testing, and due to mission degradation is a constraint. Numerical results indicate that for a given expected cost constraint, substantial weight savings and improvements of reliability can be realized by proof testing.

17. Key Words (Selected by Author(s)) Civil Engineering Interplanetary Spacecraft, Advanced Planetary Spacecraft, Advanced Structural Engineering	18. Distribution Statement Unclassified -- Unlimited

19. Security Classif. (of this report) Unclassified	20. Security Classif. (of this page) Unclassified	21. No. of Pages 34	22. Price

HOW TO FILL OUT THE TECHNICAL REPORT STANDARD TITLE PAGE

Make items 1, 4, 5, 9, 12, and 13 agree with the corresponding information on the report cover. Use all capital letters for title (item 4). Leave items 2, 6, and 14 blank. Complete the remaining items as follows:

3. Recipient's Catalog No. Reserved for use by report recipients.

7. Author(s). Include corresponding information from the report cover. In addition, list the affiliation of an author if it differs from that of the performing organization.

8. Performing Organization Report No. Insert if performing organization wishes to assign this number.

10. Work Unit No. Use the agency-wide code (for example, 923-50-10-06-72), which uniquely identifies the work unit under which the work was authorized. Non-NASA performing organizations will leave this blank.

11. Insert the number of the contract or grant under which the report was prepared.

15. Supplementary Notes. Enter information not included elsewhere but useful, such as: Prepared in cooperation with... Translation of (or by)... Presented at conference of... To be published in...

16. Abstract. Include a brief (not to exceed 200 words) factual summary of the most significant information contained in the report. If possible, the abstract of a classified report should be unclassified. If the report contains a significant bibliography or literature survey, mention it here.

17. Key Words. Insert terms or short phrases selected by the author that identify the principal subjects covered in the report, and that are sufficiently specific and precise to be used for cataloging.

18. Distribution Statement. Enter one of the authorized statements used to denote releasability to the public or a limitation on dissemination for reasons other than security of defense information. Authorized statements are "Unclassified—Unlimited, " "U.S. Government and Contractors only, " "U. S. Government Agencies only, " and "NASA and NASA Contractors only. "

19. Security Classification (of report). NOTE: Reports carrying a security classification will require additional markings giving security and down-grading information as specified by the Security Requirements Checklist and the DoD Industrial Security Manual (DoD 5220.22-M).

20. Security Classification (of this page). NOTE: Because this page may be used in preparing announcements, bibliographies, and data banks, it should be unclassified if possible. If a classification is required, indicate separately the classification of the title and the abstract by following these items with either "(U)" for unclassified, or "(C)" or "(S)" as applicable for classified items.

21. No. of Pages. Insert the number of pages.

22. Price. Insert the price set by the Clearinghouse for Federal Scientific and Technical Information or the Government Printing Office, if known.